Fourier Analysis and Function Spaces

ChE 132A handout

(Adapted from Graham and Rawlings (2022).)

1 Fourier Series — a First Look

1.1 Function Approximation

Earlier, when we solved ODEs with power series, we built solutions from the monomials $\varphi_m(x) = x^m$. Figure 1 shows the first twenty of these on $[0, 1]$. They are perfectly usable basis functions for building up the theory, but notice how they all crowd together near $x = 1$ and become hard to distinguish. That makes them quite limited in numerical application.

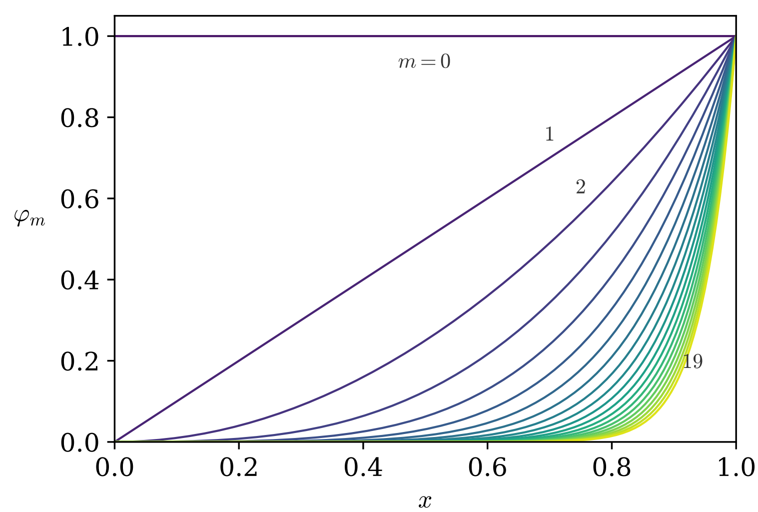

Figure 1: First twenty monomial basis functions $\varphi_m(x) = x^m$. Higher-degree monomials crowd together near $x = 1$, making them hard to distinguish and numerically ill-conditioned as a basis.

For representing general functions the *sine functions* are far better behaved, and we often use them in numerical calculations. Figure 2 shows the first ten normalized sine functions

$$\varphi_m(x) = \sqrt{2}\sin(m\pi x)$$

They oscillate uniformly across $[0, 1]$, each one varying on a different length scale, and—crucially— they are *orthogonal* to each other, meaning

$$\int_0^1 \varphi_m(x)\,\varphi_n(x)\;\mathrm{d}x = 0 \qquad m \neq n$$

We write this integral as $\langle \varphi_m, \varphi_n \rangle$, the *inner product* of φ_m and φ_n in a function space — the direct analog of the dot product (a, b) we used when a and b were vectors in a vector space

$$\langle \varphi_m, \varphi_n \rangle = 0 \qquad m \neq n$$

Next we calculate the Fourier series for representing the function $f(x) = 1 - x$.

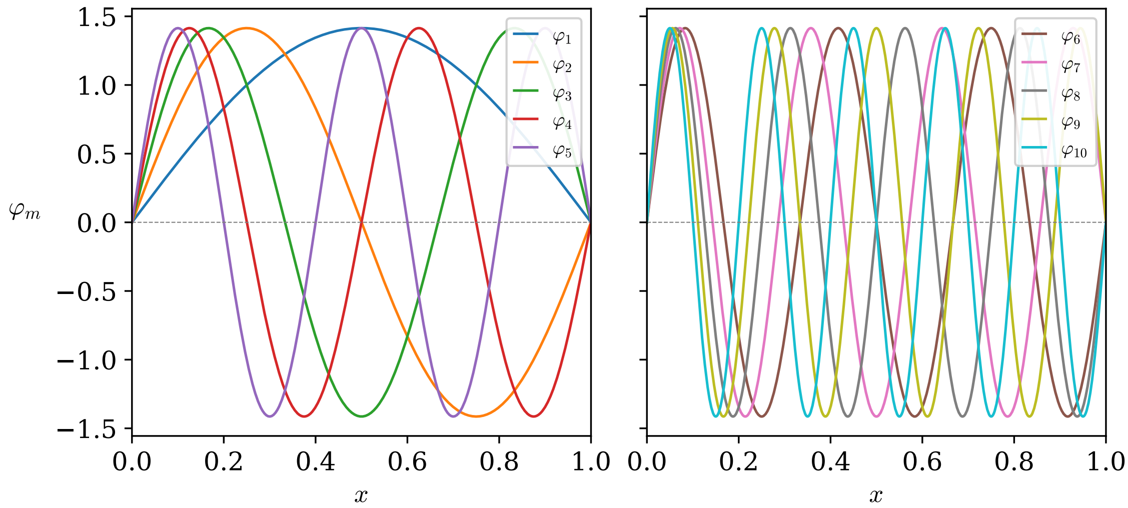

Figure 2: First ten normalized sine basis functions $\varphi_m(x) = \sqrt{2}\sin(m\pi x)$. Each function oscillates uniformly across $[0, 1]$ on its own length scale, and functions of different frequency are orthogonal to each other.

Example 1.1 (Sine series for $f(x) = 1 - x$). Represent $f(x) = 1 - x$ on $x \in [0, 1]$ as a Fourier sine series.

Step 1: an orthonormal basis. Define the functions

$$\varphi_m(x) = \sqrt{2}\,\sin(m\pi x), \qquad m = 1, 2, 3, \ldots$$

We claim these are orthonormal on $[0, 1]$ with respect to the inner product $\langle u, v\rangle = \int_0^1 u(x)\,v(x)\,\mathrm{d}x$

$$\langle \varphi_m, \varphi_n\rangle = \int_0^1 \varphi_m(x)\,\varphi_n(x)\,\mathrm{d}x = 2\int_0^1 \sin(m\pi x)\sin(n\pi x)\,\mathrm{d}x$$

Using the product-to-sum identity $2\sin A\sin B = \cos(A - B) - \cos(A + B)$

$$\langle \varphi_m, \varphi_n\rangle = \int_0^1 \left[\cos\big((m-n)\pi x\big) - \cos\big((m+n)\pi x\big)\right]\,\mathrm{d}x$$

For $m \neq n$, both integrals vanish because sine is periodic with integer period on $[0, 1]$. For $m = n$

$$\int_0^1 \cos(0)\,\mathrm{d}x - \int_0^1 \cos(2m\pi x)\,\mathrm{d}x = 1 - 0 = 1$$

Hence

$$\langle \varphi_m, \varphi_n\rangle = \begin{cases} 0 & m \neq n \\ 1 & m = n \end{cases}$$

Since this pattern of 0 for $m \neq n$ and 1 for $m = n$ appears constantly in Fourier-series calculations, we give it a name: the *Kronecker delta*

$$\delta_{mn} = \begin{cases} 0 & m \neq n \\ 1 & m = n \end{cases}$$

With this notation, the orthonormality of the sine basis is, as a compact summary,

$$\langle \varphi_m, \varphi_n\rangle = \delta_{mn}$$

Step 2: Fourier coefficients. Write $f(x) = \sum_{j=1}^{\infty} \alpha_j \, \varphi_j(x)$. To isolate a particular coefficient α_k, take the inner product of both sides with φ_k and switch the order of integration and summation to obtain

$$\langle f, \varphi_k \rangle = \left\langle \sum_{j=1}^{\infty} \alpha_j \, \varphi_j, \; \varphi_k \right\rangle = \sum_{j=1}^{\infty} \alpha_j \, \langle \varphi_j, \varphi_k \rangle$$

Writing out the sum term by term and applying orthonormality ($\langle \varphi_j, \varphi_k \rangle = 0$ for $j \neq k$; $\langle \varphi_k, \varphi_k \rangle = 1$) gives

$$\begin{aligned} \langle f, \varphi_k \rangle &= \alpha_1 \underbrace{\langle \varphi_1, \varphi_k \rangle}_{0} + \alpha_2 \underbrace{\langle \varphi_2, \varphi_k \rangle}_{0} + \cdots + \alpha_k \underbrace{\langle \varphi_k, \varphi_k \rangle}_{1} + \alpha_{k+1} \underbrace{\langle \varphi_{k+1}, \varphi_k \rangle}_{0} + \cdots \\ \langle f, \varphi_k \rangle &= \alpha_k \end{aligned}$$

So we have found the Fourier coefficients for *any* function $f(x)$

$$\boxed{\alpha_k = \langle f, \varphi_k \rangle, \quad k = 1, 2, \ldots} \qquad \text{Fourier coefficient formula} \tag{1}$$

which is a beautiful result considering that we had infinitely many α_k to determine. The critical simplification came about because we selected an *orthogonal* set of basis functions.

Next we apply this formula to calculate the Fourier coefficients for our particular $f(x) = 1 - x$ function

$$\alpha_k = \langle f, \varphi_k \rangle = \sqrt{2} \int_0^1 (1 - x) \sin(k\pi x) \; \mathrm{d}x$$

Integration by parts ($u = 1 - x$, $dv = \sin(k\pi x)\, dx$) gives

$$\int_0^1 (1 - x) \sin(k\pi x) \, dx = \left[-(1 - x) \frac{\cos(k\pi x)}{k\pi} \right]_0^1 - \int_0^1 \frac{\cos(k\pi x)}{k\pi} \, dx = \frac{1}{k\pi} - 0 = \frac{1}{k\pi}$$

Therefore

$$\alpha_k = \frac{\sqrt{2}}{k\pi} \qquad k = 1, 2, \ldots$$

Step 3: Parseval's identity. Now let's compute $\|f\|^2 = \langle f, f \rangle$ by taking the inner product of f with itself. Using the series expansion of f we have

$$\langle f, f \rangle = \left\langle \sum_{j=1}^{\infty} \alpha_j \varphi_j, \; \sum_{k=1}^{\infty} \alpha_k \varphi_k \right\rangle = \sum_{j=1}^{\infty} \alpha_j \sum_{k=1}^{\infty} \alpha_k \, \langle \varphi_j, \varphi_k \rangle$$

where we have again switched the order of integration and summation (twice). Performing the inner sum over k for fixed j gives

$$\sum_{k=1}^{\infty} \alpha_k \, \langle \varphi_j, \varphi_k \rangle = \alpha_1 \underbrace{\langle \varphi_j, \varphi_1 \rangle}_{0} + \cdots + \alpha_j \underbrace{\langle \varphi_j, \varphi_j \rangle}_{1} + \alpha_{j+1} \underbrace{\langle \varphi_j, \varphi_{j+1} \rangle}_{0} + \cdots \; = \; \alpha_j$$

Substituting this result back into the outer sum gives

$$\langle f, f \rangle = \sum_{j=1}^{\infty} \alpha_j \alpha_j = \sum_{j=1}^{\infty} \alpha_j^2$$

and we have derived a formula for $\|f\|^2$ known as Parseval's identity

$$\boxed{\|f\|^2 = \sum_{j=1}^{\infty} \alpha_j^2} \qquad \text{Parseval's identity} \tag{2}$$

Applying (2) to the present example

$$\|f\|^2 = \int_0^1 (1-x)^2\,dx = \sum_{k=1}^{\infty} \frac{2}{k^2\pi^2}$$

Performing the integral gives $1/3$, so we have shown[1]

$$\sum_{k=1}^{\infty} \frac{1}{k^2} = \frac{\pi^2}{6}$$

Step 4: partial sums. The N-term approximation is

$$f_N(x) = \sum_{k=1}^{N} \frac{2}{k\pi} \sin(k\pi x)$$

Figure 3 shows $f(x)$ and $f_N(x)$ for increasing N. Note the slow convergence near $x = 0$: all sine functions vanish at $x = 0$, while $f(0) = 1$, so a large number of terms is needed to approximate that corner.

1.2 Solving Differential Equations

Another major application of Fourier series is to solve linear differential equations (both PDEs and ODEs). We illustrate by solving the heat equation, which was Fourier's original interest leading to his development of the Fourier series.

Example 1.2 (Steady-state heat equation solved by Fourier series)**.** The transient heat equation for a one-dimensional rod with internal heat generation $F(x)$ in $x \in [0, 1]$, $t \geq 0$ is

$$\rho C_p \frac{\partial T}{\partial t} = k \frac{\partial^2 T}{\partial x^2} + F(x)$$

Here ρ is the material density, C_p the heat capacity, and k the thermal conductivity. We defer the transient (PDE) problem to a later section, and here solve the steady-state problem. Setting $\partial T/\partial t = 0$ and dividing by k gives the steady-state ODE

$$T'' = -f(x), \qquad T(0) = 0, \quad T(1) = 0 \tag{3}$$

[1] Recall in the math background section on series at the start of the course, I showed that the ratio test fails on both of these series

$$S_1 = 1 + \frac{1}{2} + \frac{1}{3} + \frac{1}{4} + \cdots$$
$$S_2 = 1 + \frac{1}{2^2} + \frac{1}{3^2} + \frac{1}{4^2} + \cdots$$

and I mentioned that the first series diverges, but the second one converges to $\ldots \pi^2/6$. And you laughed. So now we know where that $\pi^2/6$ comes from!

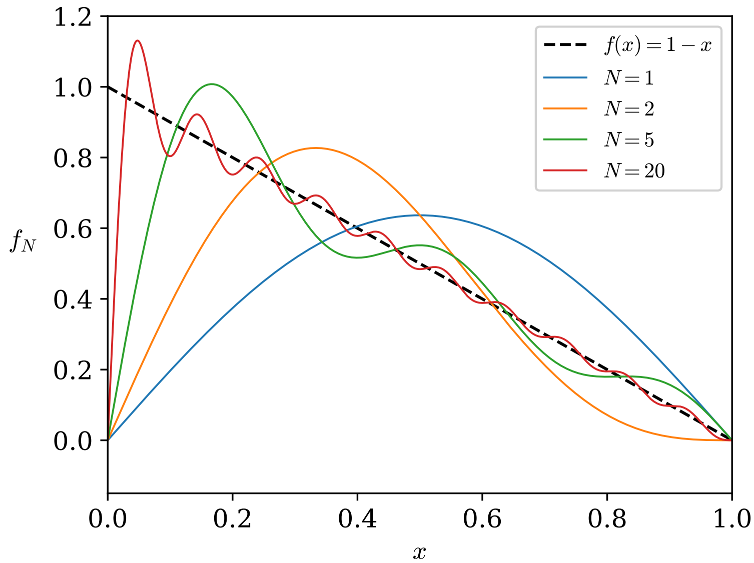

Figure 3: Partial sums $f_N(x) = \sum_{k=1}^{N} \frac{2}{k\pi} \sin(k\pi x)$ approximating $f(x) = 1 - x$ (dashed).

where $f(x) \equiv F(x)/k$. (We will handle nonzero boundary temperatures shortly.)

Expanding in the sine basis. Use the orthonormal sine basis $\varphi_n(x) = \sqrt{2}\sin(n\pi x)$ from Example 1.1, and expand *both* $f(x)$ and the unknown $T(x)$

$$f(x) = \sum_{n=1}^{\infty} b_n \, \varphi_n(x), \qquad b_n = \langle f, \varphi_n \rangle = \sqrt{2} \int_0^1 f(x) \sin(n\pi x) \, \mathrm{d}x$$

$$T(x) = \sum_{n=1}^{\infty} a_n \, \varphi_n(x)$$

Solving for the coefficients. Because $\varphi_n''(x) = -n^2\pi^2 \, \varphi_n(x)$, differentiating the series for T twice gives

$$T''(x) = \sum_{n=1}^{\infty} a_n \, \varphi_n''(x) = -\sum_{n=1}^{\infty} n^2\pi^2 \, a_n \, \varphi_n(x)$$

Substituting into (3) and collecting all terms over the common basis $\{\varphi_n\}$

$$\sum_{n=1}^{\infty} \left(b_n - n^2\pi^2 \, a_n\right) \varphi_n(x) = 0$$

The only way for this series to equal the zero function is if every coefficient in brackets vanishes individually

$$b_n - n^2\pi^2 \, a_n = 0$$

Solving for a_n

$$a_n = \frac{b_n}{n^2\pi^2}, \quad n = 1, 2, \ldots$$

The solution is therefore

$$T(x) = \sum_{n=1}^{\infty} \frac{b_n}{n^2\pi^2}\,\varphi_n(x) = \frac{\sqrt{2}}{\pi^2}\sum_{n=1}^{\infty} \frac{b_n}{n^2}\,\sin(n\pi x) \tag{4}$$

Verification. Differentiating (4) twice gives $T'' = -\sum_n b_n\varphi_n(x) = -f(x)$, so the ODE is satisfied. Both boundary conditions hold because $\varphi_n(0) = \varphi_n(1) = 0$ for every integer n.

The sine basis is ideally suited to this problem: the basis functions automatically satisfy the homogeneous Dirichlet boundary conditions, reducing the boundary-value problem to a simple algebraic relation among Fourier coefficients.

Example 1.3 (Nonhomogeneous boundary conditions)**.** Now consider the same ODE but with nonzero boundary temperatures

$$T'' = -f(x), \qquad T(0) = \alpha, \quad T(1) = \beta \tag{5}$$

Particular solution by inspection. We look for a *particular solution* $T_p(x)$ that satisfies the *homogeneous* form of the ODE,

$$T_p'' = 0$$

but satisfies the *nonhomogeneous* boundary values $T_p(0) = \alpha$, $T_p(1) = \beta$. By inspection,

$$T_p(x) = \alpha(1-x) + \beta x$$

satisfies both requirements: its second derivative is identically zero, and $T_p(0) = \alpha$, $T_p(1) = \beta$.

Superposition. Write the full solution as

$$T(x) = T_{\text{hg}}(x) + T_p(x)$$

where T_{hg} is the homogeneous-BC solution from Example 1.2, which satisfies

$$T_{\text{hg}}'' = -f(x), \qquad T_{\text{hg}}(0) = 0, \quad T_{\text{hg}}(1) = 0$$

Substituting into (5) verifies every requirement

$$\begin{aligned} T'' &= T_{\text{hg}}'' + T_p'' = -f(x) + 0 = -f(x) \\ T(0) &= T_{\text{hg}}(0) + T_p(0) = 0 + \alpha = \alpha \\ T(1) &= T_{\text{hg}}(1) + T_p(1) = 0 + \beta = \beta \end{aligned}$$

The complete solution is therefore

$$T(x) = \sum_{n=1}^{\infty} \frac{b_n}{n^2\pi^2}\,\varphi_n(x) + \alpha(1-x) + \beta x \tag{6}$$

Example 1.4 (Numerical solution: $f(x) = 1-x$, $\alpha = 0.1$, $\beta = -0.1$)**.** Take $f(x) = 1-x$ (i.e., $F(x) = k(1-x)$) with boundary temperatures $\alpha = 0.1$, $\beta = -0.1$.

Fourier coefficients. In Example 1.1 we computed the Fourier coefficients of $f(x) = 1-x$ in the orthonormal sine basis

$$b_n = \langle f, \varphi_n\rangle = \frac{\sqrt{2}}{n\pi}$$

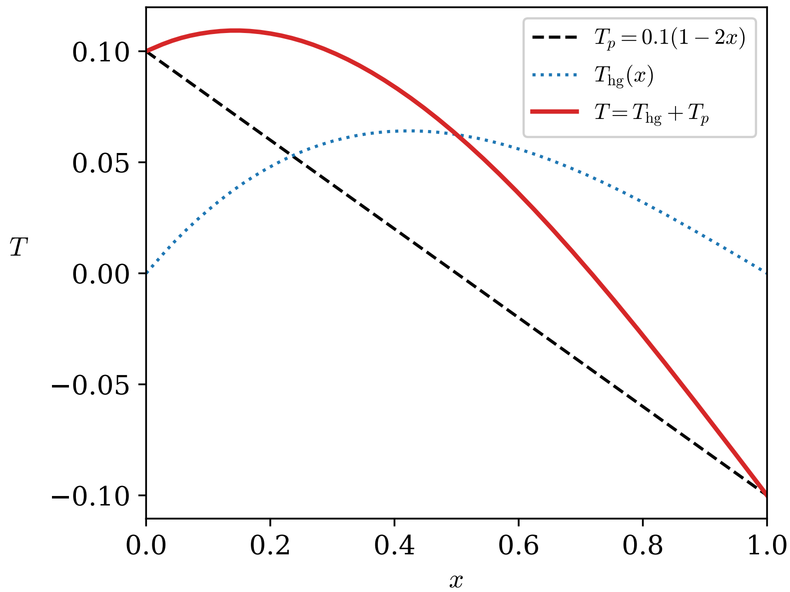

Figure 4: Steady-state temperature with $f(x) = 1 - x$, $\alpha = 0.1$, $\beta = -0.1$. Dashed: particular solution $T_p = 0.1(1 - 2x)$. Dotted: Fourier part T_{hg} (homogeneous BCs). Solid: full solution $T = T_{hg} + T_p$.

From Example 1.2, $a_n = b_n/(n^2\pi^2)$, giving

$$a_n = \frac{\sqrt{2}}{n^3\pi^3}$$

Solution. The homogeneous-BC part is

$$T_{hg}(x) = \sum_{n=1}^{\infty} a_n\, \varphi_n(x) = \frac{2}{\pi^3} \sum_{n=1}^{\infty} \frac{\sin(n\pi x)}{n^3}$$

and the particular solution is $T_p(x) = 0.1(1 - 2x)$. The complete solution is

$$T(x) = \frac{2}{\pi^3} \sum_{n=1}^{\infty} \frac{\sin(n\pi x)}{n^3} + 0.1(1 - 2x) \tag{7}$$

which satisfies $T'' = -(1 - x)$, $T(0) = 0.1$, $T(1) = -0.1$. Because the coefficients decay as $1/n^3$, the series converges rapidly and five terms are already visually indistinguishable from the exact result.

Figure 4 shows the three components. The particular solution $T_p = 0.1(1 - 2x)$ is a small declining ramp from 0.1 to −0.1; the Fourier part T_{hg} is a positive arch (peak $\approx 2/\pi^3 \approx 0.06$) reflecting the internal heat generation; the full solution T is their sum, with the arch clearly visible as a departure from the ramp.

2 Bessel Functions

A second-order ODE that arises frequently in transport problems (heat conduction, diffusion, fluid flow) is

$$\nabla^2 y \pm y = 0 \tag{8}$$

This equation arises with either sign, so we treat both signs here. As you will work out in your upcoming transport classes, for a one-dimensional problem, using x for rectangular geometry and r for cylindrical or spherical geometry, the three forms are

$$\frac{d^2y}{dx^2} \pm y = 0 \qquad \text{(rectangular)}$$

$$\frac{1}{r}\frac{d}{dr}\left(r\frac{dy}{dr}\right) \pm y = 0 \qquad \text{(cylindrical)}$$

$$\frac{1}{r^2}\frac{d}{dr}\left(r^2\frac{dy}{dr}\right) \pm y = 0 \qquad \text{(spherical)}$$

These are the equations heading each column of Table 1.

Rectangular. In rectangular coordinates (rectangular) simply becomes $y'' \pm y = 0$. We know these solutions well. For the + sign the characteristic equation is $\lambda^2 + 1 = 0$, giving the two linearly independent solutions

$$\cos x \quad \text{and} \quad \sin x \qquad (+\text{ sign})$$

For the − sign the characteristic equation is $\lambda^2 - 1 = 0$, giving

$$e^x \quad \text{and} \quad e^{-x} \qquad (-\text{ sign})$$

These are the four functions in the left column of Table 1.

Spherical. The spherical ODE (spherical) can be reduced to the rectangular one by the substitution $u(r) = r\,y(r)$, i.e., $y = u/r$. Differentiating gives

$$y' = \frac{u'}{r} - \frac{u}{r^2}$$

Multiplying through by r^2

$$r^2 y' = ru' - u$$

and differentiating once more

$$\frac{d}{dr}(r^2 y') = ru''$$

Substituting into the spherical ODE (spherical) gives

$$\frac{ru''}{r^2} \pm \frac{u}{r} = 0$$

and multiplying through by r gives

$$u'' \pm u = 0$$

which is exactly the rectangular equation (rectangular). Since $y = u/r$, the four solutions in spherical coordinates are the rectangular solutions divided by r

$$\frac{\cos r}{r} \quad \text{and} \quad \frac{\sin r}{r} \qquad (+\text{ sign})$$

$$\frac{e^r}{r} \quad \text{and} \quad \frac{e^{-r}}{r} \qquad (-\text{ sign})$$

These are the four functions in the right column of Table 1.

Rectangular Coordinates	Cylindrical Coordinates	Spherical Coordinates
$\dfrac{d^2y}{dx^2} \pm y = 0$	$\dfrac{1}{r}\dfrac{d}{dr}(r\dfrac{dy}{dr}) \pm y = 0$	$\dfrac{1}{r^2}\dfrac{d}{dr}(r^2\dfrac{dy}{dr}) \pm y = 0$

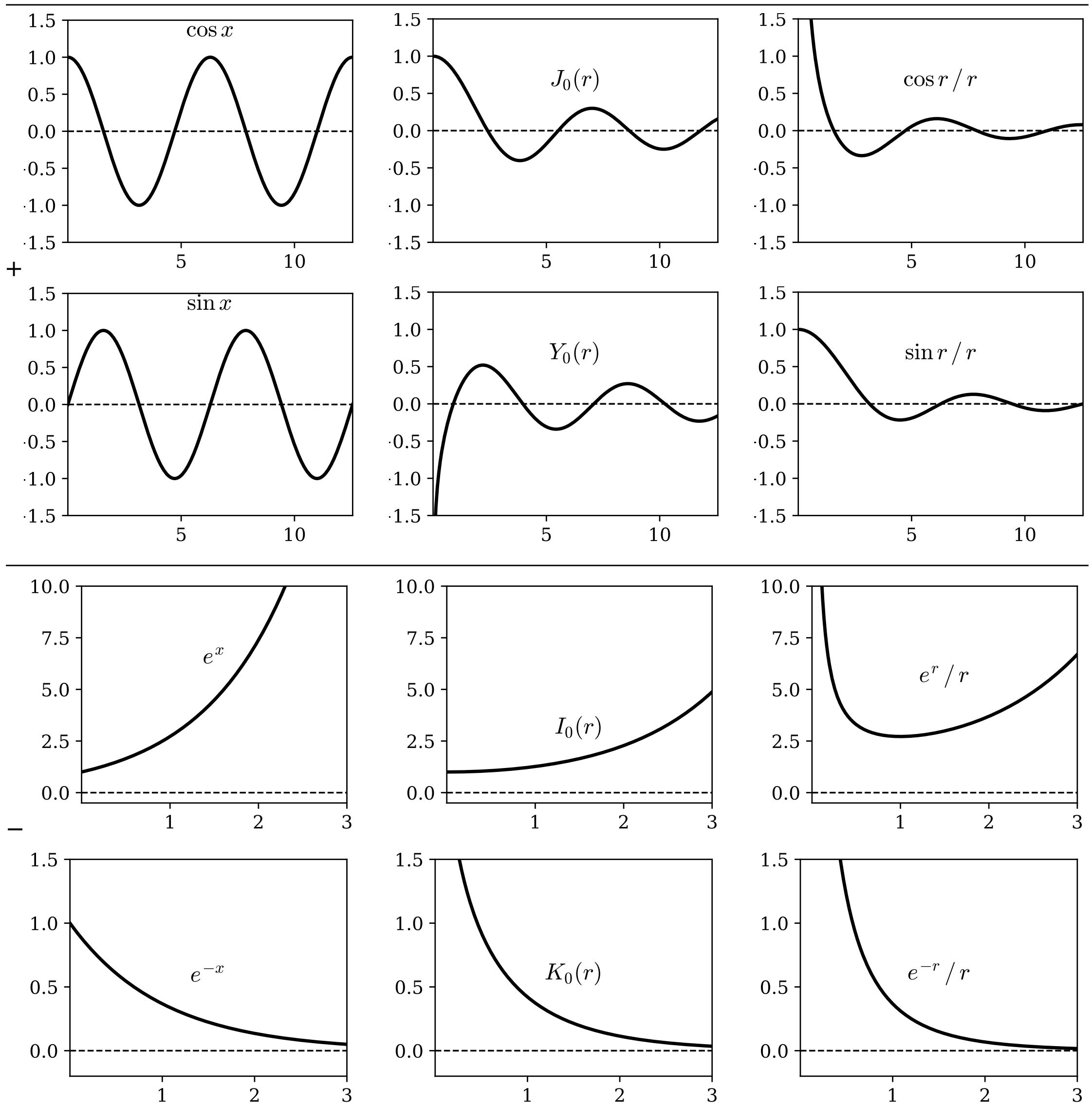

Table 1: The linear differential equations arising from the radial part of $\nabla^2 y \pm y = 0$ in rectangular, cylindrical, and spherical coordinates. Bessel functions (J_0, Y_0) and modified Bessel functions (I_0, K_0) are two linearly independent solutions in cylindrical coordinates for the plus and minus signs, respectively. The solutions in spherical coordinates are called spherical Bessel functions. Adapted from (Graham and Rawlings, 2022, Table 2.3).

Cylindrical. There are no special tricks that allow us to convert the cylindrical ODE (cylindrical) into the rectangular form. This equation requires the introduction of entirely new functions: the *Bessel functions*.

For the + sign the two linearly independent solutions are called $J_0(r)$ and $Y_0(r)$, shown in the top half of the middle column of Table 1. J_0 is the *Bessel function of the first kind, order zero*; Y_0 is the *Bessel function of the second kind, order zero*. Note that Y_0 diverges logarithmically as $r \to 0$, so it is excluded from any problem whose domain includes the origin.

For the − sign the two linearly independent solutions are called $I_0(r)$ and $K_0(r)$, shown in the bottom half of the middle column of Table 1. I_0 is the *modified Bessel function of the first kind, order zero*; K_0 is the *modified Bessel function of the second kind, order zero*. As with Y_0, the function K_0 diverges at $r = 0$ and is excluded when the domain includes the origin.

Order. If we take the derivatives given in the cylindrical form of $\nabla^2 y \pm y = 0$ and multiply by r, we obtain

$$r^2 y'' + r y' \pm r^2 y = 0$$

Generalizing, we obtain a Bessel function of *order* ν by subtracting the term $\nu^2 y$ from the left-hand side giving the *Bessel equation*

$$r^2 y'' + r y' + (\pm r^2 - \nu^2)\, y = 0, \qquad \nu \geq 0 \tag{9}$$

Two linearly independent solutions are denoted $J_\nu(r)$ and $Y_\nu(r)$ (first and second kind) for the positive sign, and the modified counterparts $I_\nu(r)$ and $K_\nu(r)$ for the minus sign. Our cylindrical ODE is the $\nu = 0$ special case, and the differentiation rules below involve the $\nu = 1$ functions J_1, Y_1, I_1, K_1.

Comparing the three columns of Table 1, notice both the similarities and the differences. The oscillatory character of $\cos x$, $\sin x$ in rectangular coordinates is mirrored by the oscillations of J_0 and Y_0 in cylindrical coordinates, but the cylindrical solutions decay in amplitude as r increases — a consequence of energy spreading outward in two dimensions rather than one. Likewise, the exponentially growing and decaying solutions $e^{\pm x}$ of the − sign problem in rectangular coordinates have their cylindrical analogs in I_0 and K_0, which grow and decay much more rapidly. The spherical solutions are simply the rectangular ones divided by r, reflecting the additional geometric decay in three dimensions.

Differentiation rules and power series. If we think of these Bessel functions the same way we think about sin, cos, and the exponential, we can expect all the usual facts to carry over. For differentiation, the simplest rules are

$$\frac{d}{dr} J_0(r) = -J_1(r), \qquad \frac{d}{dr} Y_0(r) = -Y_1(r), \tag{10}$$

$$\frac{d}{dr} I_0(r) = I_1(r), \qquad \frac{d}{dr} K_0(r) = -K_1(r) \tag{11}$$

where J_1, Y_1, I_1, K_1 are the order-1 analogs of each function, exactly as $\cos = (\sin)'$ and $\sinh = (\cosh)'$.

We can also derive power series as we did for sine and cosine, though they require a little more care because Y_0 and K_0 are singular at $r = 0$ (note their blow-up in Table 1). The series for the two non-singular functions are

$$J_0(r) = \sum_{n=0}^{\infty} \frac{(-1)^n}{(n!)^2} \left(\frac{r}{2}\right)^{2n}, \qquad I_0(r) = \sum_{n=0}^{\infty} \frac{1}{(n!)^2} \left(\frac{r}{2}\right)^{2n} \tag{12}$$

Note that I_0 is simply J_0 with the signs of alternate terms flipped — exactly the relationship cosh bears to cos. The singular functions Y_0 and K_0 include a $\ln r$ term, which is the source of their singularity at $r = 0$.

Useful small- and large-argument formulas. Truncating the J_0 and I_0 series above through second order in r, and reading the leading term of the J_1 and I_1 series (which begin at order r), gives the small-argument forms

$$J_0(r) \approx 1 - \tfrac{r^2}{4}, \qquad I_0(r) \approx 1 + \tfrac{r^2}{4}, \qquad J_1(r) \approx \tfrac{r}{2}, \qquad I_1(r) \approx \tfrac{r}{2} \tag{13}$$

In particular $J_1(r)/r \to 1/2$ and $I_1(r)/r \to 1/2$ as $r \to 0$, limits that arise routinely when applying boundedness conditions at the axis of a cylinder. The singular partners diverge logarithmically, $Y_0(r) \sim (2/\pi)\ln r$ and $K_0(r) \sim -\ln r$ as $r \to 0$.

For large argument, the four cylindrical Bessel functions of order ν have the leading asymptotic forms

$$\begin{aligned} J_\nu(r) &\sim \sqrt{\tfrac{2}{\pi r}}\,\cos\!\left(r - \tfrac{\nu\pi}{2} - \tfrac{\pi}{4}\right), \quad & I_\nu(r) &\sim \frac{e^r}{\sqrt{2\pi r}} \\ Y_\nu(r) &\sim \sqrt{\tfrac{2}{\pi r}}\,\sin\!\left(r - \tfrac{\nu\pi}{2} - \tfrac{\pi}{4}\right), \quad & K_\nu(r) &\sim \sqrt{\tfrac{\pi}{2r}}\,e^{-r} \end{aligned} \tag{14}$$

The J_ν, Y_ν pair oscillates with slowly decaying amplitude $\sim r^{-1/2}$, exactly as the cosine/sine pair does in two dimensions versus one. The modified pair I_ν, K_ν grows and decays exponentially. At leading order the modified asymptotics do not depend on ν, a fact used in Exercise 8 when taking the high-Thiele-modulus limit of the catalyst effectiveness factor.

A thorough tabulation of all such formulas — differentiation identities, recurrence relations, integral representations, asymptotic expansions, and zeros — is given in Abramowitz and Stegun (1964), the standard reference for special functions.

Numerical support. Numerical support for Bessel functions is excellent in all major scientific computing environments. Table 2 shows the naming conventions for the cylindrical functions in two popular languages, together with the figure they produce.

3 Function Spaces and Differential Operators

3.1 Functions as Vectors

In Section 1 we used the inner product $\langle u, v\rangle = \int_0^1 u(x)\,v(x)\,\mathrm{d}x$ to project a function onto each basis sine. This was not just a clever device — it is the function-space version of the dot product, and *all* of our intuition about vectors carries over.

In the finite-dimensional space $\mathbb{R}^n$, the dot product of two vectors a and b is

$$(a, b) = \sum_{i=1}^{n} a_i\, b_i$$

For real functions $u(x)$ and $v(x)$ on a domain $a \le x \le b$, the natural analog is

$$\langle u, v\rangle = \int_a^b u(x)\,v(x)\,\mathrm{d}x$$

We use the angle-bracket notation $\langle\,\cdot\,,\,\cdot\,\rangle$ to distinguish the inner product of *functions* from the dot product $(\,\cdot\,,\,\cdot\,)$ of vectors. From this inner product we obtain a norm

$$\|u\| = \sqrt{\langle u, u\rangle} = \left[\int_a^b u(x)^2\,\mathrm{d}x\right]^{1/2}$$

Python (NumPy / SciPy)

```
import numpy as np
import matplotlib.pyplot as plt
from scipy.special import jn, yn, iv, kv

r  = np.linspace(1e-6, 4*np.pi, 200)
rs = np.linspace(1e-6, 3, 200)
fig, ax = plt.subplots(2, 2)
ax[0,0].plot(r,  jn(0,r))
ax[0,0].set_title('J0')
ax[0,1].plot(r,  yn(0,r))
ax[0,1].set_title('Y0')
ax[1,0].plot(rs, iv(0,rs))
ax[1,0].set_title('I0')
ax[1,1].plot(rs, kv(0,rs))
ax[1,1].set_title('K0')
plt.tight_layout()
plt.savefig('bessel_cyl.pdf')
```

Matlab/Octave

```
r  = linspace(1e-6, 4*pi, 200);
rs = linspace(1e-6, 3, 200);
subplot(2,2,1)
plot(r,  besselj(0,r))
title('J0')
subplot(2,2,2)
plot(r,  bessely(0,r))
title('Y0')
subplot(2,2,3)
plot(rs, besseli(0,rs))
title('I0')
subplot(2,2,4)
plot(rs, besselk(0,rs))
title('K0')
```

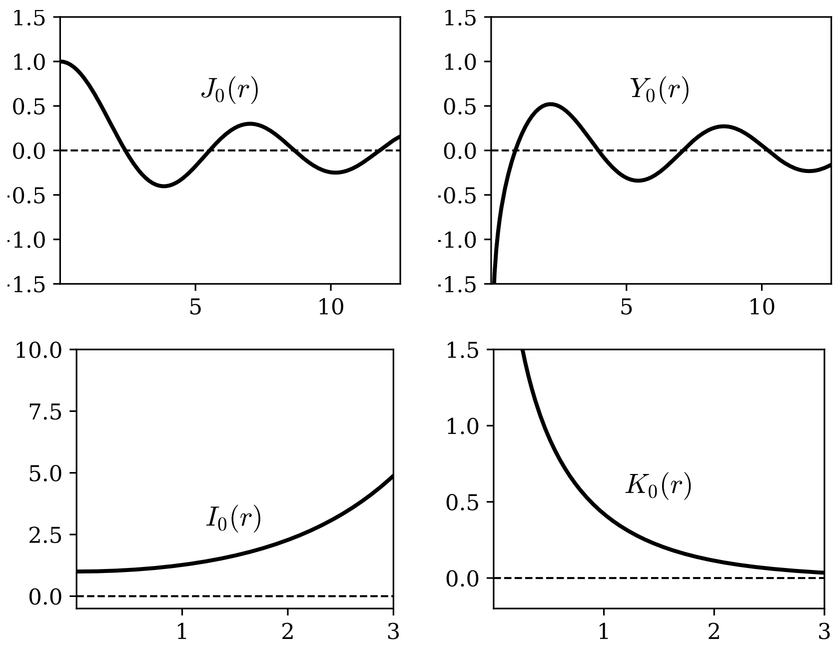

Table 2: Cylindrical Bessel functions J_0, Y_0, I_0, K_0 (the middle column of Table 1), together with Python and Matlab code that produces this figure. In NumPy/SciPy the functions are `jn(0,r)`, `yn(0,r)`, `iv(0,r)`, `kv(0,r)`; in Matlab they are `besselj`, `bessely`, `besseli`, `besselk`.

We will sometimes also need a *weighted* inner product

$$\langle u, v\rangle_w = \int_a^b u(x)\, v(x)\, w(x)\; \mathrm{d}x$$

where $w(x) > 0$ on (a, b) is a weight function. We will see shortly that the natural inner product for the Bessel basis on $(0, l)$ is weighted by $w(x) = x$.

These definitions produce an honest infinite-dimensional vector space: angles, lengths, projections, and orthogonality all behave just as they do in two or three dimensions. *All of our intuition about directions, lengths, and angles carries over from two dimensions into an infinite number of dimensions.* Mathematicians call this a HILBERT SPACE; we will not need any more vocabulary than that.

Basis Sets and Fourier Series. In a finite-dimensional space, any vector can be represented in an orthonormal basis $\{e_1, e_2, \ldots, e_n\}$ as

$$a = \sum_{i=1}^{n} (a, e_i)\, e_i$$

The same is true in a function space, except that each basis vector is now a function $\varphi_n(x)$ and the sum is infinite

$$f(x) = \sum_{n=1}^{\infty} \alpha_n\, \varphi_n(x), \qquad \alpha_n = \langle f, \varphi_n\rangle \tag{15}$$

This is exactly the formula we derived in Example 1.1 for the sine basis on $[0, 1]$ — only now we recognize it as a general fact: for *any* orthonormal basis $\{\varphi_n\}$ of a function space, the coefficients of any function f in that basis are obtained by inner-product projection.

Beyond the sine basis we used in Section 1, two other important bases are the Legendre polynomials and the Bessel functions, which we examine in turn.

Truncation and the residual. The infinite series (15) is fine in principle, but in practice we always work with the truncated series

$$f_N(x) = \sum_{n=1}^{N} \alpha_n\, \varphi_n(x)$$

The Fourier coefficients have a remarkable optimality property: among *all* possible coefficient choices in the truncated sum, the values $\alpha_n = \langle f, \varphi_n\rangle$ minimize the residual norm

$$\|f - f_N\|^2 = \int_a^b \big(f(x) - f_N(x)\big)^2\; \mathrm{d}x$$

The intuition is the same as in finite dimensions: projecting a vector onto a subspace minimizes the perpendicular distance, and the inner-product formula is exactly that orthogonal projection. An immediate practical consequence is that the coefficients α_n do not depend on N; if we decide to add more terms, we do not need to recompute the ones we already have.

How fast does the series converge? The rate at which $f_N \to f$ depends on the smoothness of f and on how well its boundary values match the basis functions:

- If f and all its derivatives are smooth and periodic — so the function and basis agree at the boundaries to all orders — then the coefficients α_n decay faster than any power of n^{-1}. This is called SPECTRAL or exponential convergence.
- If f has a jump discontinuity, or if f is smooth in the interior but its boundary values disagree with the basis (the basis is "implicitly periodic" but f is not), then α_n decays only as n^{-1} and the partial sums oscillate near the discontinuity. These oscillations are called the GIBBS PHENOMENON.

We saw the slow case already in Example 1.1: for $f(x) = 1 - x$ on $[0, 1]$, the sine coefficients $\alpha_k = \sqrt{2}/(k\pi)$ decay like $1/k$ and Figure 3 shows the slow approach to $f(0) = 1$ because every basis sine vanishes at $x = 0$.

Rescaling to a different interval. Real problems are rarely posed on $[0, 1]$ exactly — a heat-equation rod might have length L and live on $[0, L]$. Once a basis works on a reference interval, we adapt it to any other by a simple change of variable. For example, the sine basis $\sin(n\pi x)$ on $[0, 1]$ rescales to $\sin(n\pi x/L)$ on $[0, L]$. We will work the remainder of this section on the standard intervals $[0, 1]$ and $[-1, 1]$ to keep the formulas clean, with the understanding that any real problem is just a rescaling away.

Example: a Gaussian on $[-1, 1]$ in the (rescaled) sine basis. For an example of fast convergence, take the smooth Gaussian

$$f(x) = \exp(-8\,x^2)$$

on $[-1, 1]$. The sine basis from Section 1 lives on $[0, 1]$, but the rescaling above moves it to $[-1, 1]$: setting $y = (x + 1)/2$ maps $x \in [-1, 1]$ to $y \in [0, 1]$, so the basis $\sin(n\pi y)$ on $[0, 1]$ becomes

$$\varphi_n(x) = \sin\left(\frac{n\pi(x+1)}{2}\right), \qquad n = 1, 2, 3, \ldots$$

on $[-1, 1]$. Each φ_n vanishes at both endpoints $x = \pm 1$ and the same change-of-variable shows that the φ_n are orthonormal on $[-1, 1]$: $\langle \varphi_m, \varphi_n \rangle = \delta_{mn}$.

The Gaussian $f(x) = \exp(-8x^2)$ is essentially zero at both endpoints ($\exp(-8) \approx 3 \times 10^{-4}$), so its boundary values match the basis and there is no Gibbs penalty. Figure 5 shows the truncated series $f_N(x) = \sum_{n=1}^{N} b_n\, \varphi_n(x)$ for $N = 2, 5, 10$: by $N = 5$ the approximation is already visually indistinguishable from the exact function — spectral convergence in action.

3.2 Fixing those Pesky Monomials — Legendre Polynomials

In Section 1 (Figure 1) we saw that the simple monomial basis $\{1, x, x^2, \ldots\}$ is unsuitable for numerical work because the higher-degree monomials crowd together near the boundary. The monomials are also *not* orthogonal on $[-1, 1]$. In fact, since they are all positive functions, none of their inner products are zero, and none of them are orthogonal to each other.

It is, however, possible to take linear combinations of the monomials and produce an *orthogonal* polynomial basis on $[-1, 1]$. The resulting polynomials are called the Legendre polynomials, $P_n(x)$. The first four are

$$P_0(x) = 1 \tag{16}$$
$$P_1(x) = x \tag{17}$$
$$P_2(x) = \tfrac{1}{2}(3x^2 - 1) \tag{18}$$
$$P_3(x) = \tfrac{1}{2}(5x^3 - 3x) \tag{19}$$

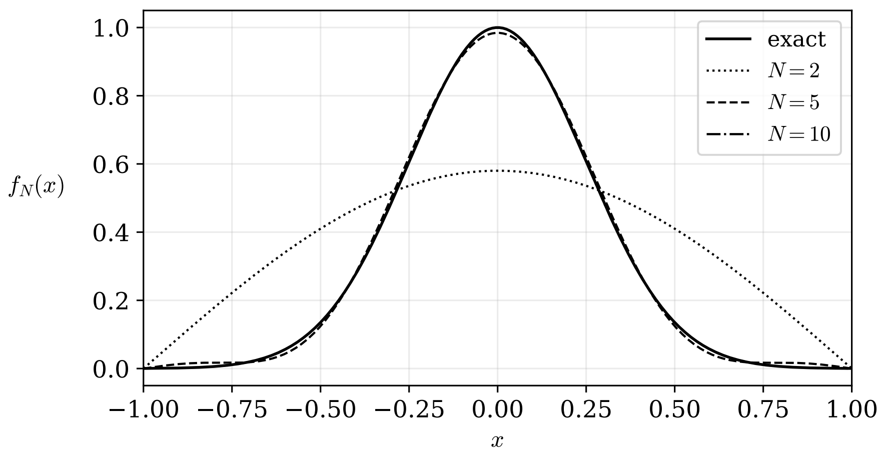

Figure 5: Function $f(x) = \exp(-8x^2)$ on $[-1, 1]$ and truncated sine-basis approximations $f_N(x) = \sum_{n=1}^{N} b_n \sin\big(n\pi(x+1)/2\big)$ with $N = 2, 5, 10$. The approximation with $N = 5$ is already visually indistinguishable from the exact function (and $N = 10$ is on top of it).

and the rest are generated efficiently by the three-term recurrence

$$(n+1)\,P_{n+1}(x) = (2n+1)\,x\,P_n(x) - n\,P_{n-1}(x) \tag{20}$$

Figure 6 shows the first ten of these, in the same style as the monomial basis (Figure 1) and the sine basis (Figure 2). Notice how the Legendre polynomials oscillate on different length scales across $[-1, 1]$ — much like the sine basis — but their amplitude is 1 at the endpoints rather than 0, so they can represent functions that take arbitrary values there.

These polynomials are orthogonal — but *not* orthonormal — with respect to the standard inner product on $[-1, 1]$. By convention each P_n is scaled so that $P_n(1) = 1$, which gives the normalization

$$\langle P_m, P_n \rangle = \int_{-1}^{1} P_m(x)\,P_n(x)\;\mathrm{d}x = \frac{2}{2n+1}\,\delta_{mn} \tag{21}$$

The Fourier–Legendre series of a function f on $[-1, 1]$ is therefore

$$f(x) = \sum_{n=0}^{\infty} a_n\,P_n(x), \qquad a_n = \frac{2n+1}{2}\,\langle f, P_n \rangle = \frac{2n+1}{2} \int_{-1}^{1} f(x)\,P_n(x)\;\mathrm{d}x \tag{22}$$

Note that the sum starts with the index $n = 0$, which is conventional for polynomial bases.

Example 3.1 (Legendre series of $f(x) = 1 - x$ on $[-1, 1]$)**.** The function $1 - x$ is itself a polynomial of degree 1, so its Legendre series can be read off by inspection: $1 - x = P_0(x) - P_1(x)$, hence

$$a_0 = 1, \qquad a_1 = -1, \qquad a_n = 0 \quad \text{for } n \geq 2$$

The series terminates exactly in two terms. Compare this with the sine series of the same function on $[0, 1]$ in Example 1.1, which required infinitely many terms and converged slowly near $x = 0$. The Legendre basis fits the linear function naturally because there is no implicit periodicity assumption to violate.

Example 3.2 (Legendre series of $f(x) = \exp(-8x^2)$ on $[-1, 1]$)**.** This Gaussian is smooth and even, so all odd coefficients vanish. We compute the even coefficients numerically using (22), giving the truncated approximations shown in Figure 7 for $N = 2, 5, 10$. Convergence is spectral — by $N = 5$ the approximation is visually indistinguishable from the exact function.

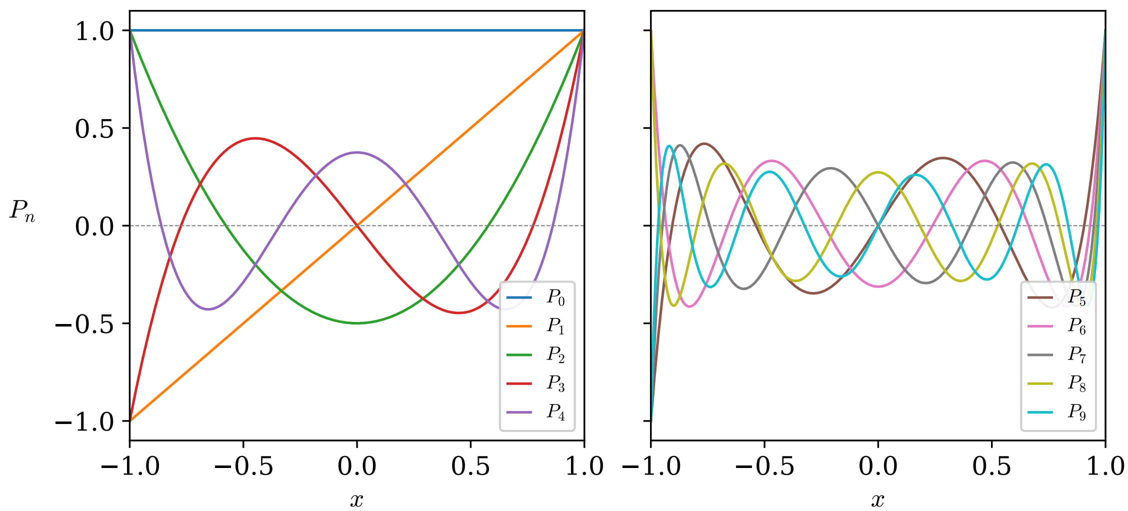

Figure 6: First ten Legendre polynomials $P_0, P_1, \ldots, P_9$ on $[-1, 1]$. Each oscillates uniformly across the interval on its own length scale, and all are normalized so that $P_n(1) = 1$. Polynomials of different degree are orthogonal to each other.

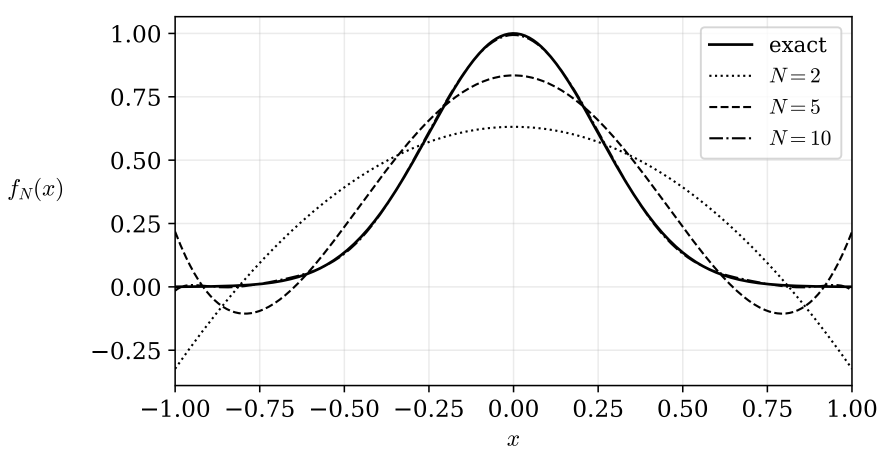

Figure 7: Function $f(x) = \exp(-8x^2)$ and truncated Legendre–Fourier series approximations with $N = 2, 5, 10$.

The trigonometric and Legendre basis sets are very important, but there are many others that also are important and widely seen in applications. Why do all these orthogonal bases exist? The unifying answer is that each one arises as the eigenfunctions of a special class of differential operator, which we introduce in the next section.

3.3 Eigenfunctions of Differential Operators

We have discussed two orthogonal bases — sines and Legendre polynomials — and the natural question is, can we generalize this idea further? What makes these families orthogonal in the first place? The answer is that each one is the set of *eigenfunctions of a differential operator*. We introduce that concept now and work it out in detail for the sines, and then use the same machinery to discover a third basis (Bessel functions).

Recall: eigenvectors of matrices. From linear algebra, a square matrix A has special *nonzero* vectors $\mathbf{v}$ that are only rescaled by matrix multiplication

$$A\mathbf{v} = \lambda\,\mathbf{v}$$

The vector $\mathbf{v}$ is an *eigenvector* of A and the scalar λ is the corresponding *eigenvalue*. When A is symmetric ($A^T = A$), the eigenvectors are mutually orthogonal and form a basis of $\mathbb{R}^n$, so any vector can be expanded in the eigenvector basis with coefficients given by inner-product projections.

Same idea for differential operators. A *differential operator* L takes a function and produces another function. The simplest example, and the one we focus on first, is the second derivative, $L = d^2/dx^2$, which sends $u(x)$ to $u''(x)$. An *eigenfunction* of L is a nontrivial function u that L scales,

$$Lu + \lambda u = 0 \tag{23}$$

i.e., $Lu = -\lambda u$.[2] The function u is the *eigenfunction* and λ is the corresponding *eigenvalue*.

The remarkable fact, which we are about to verify in our running example, is that the eigenfunctions of the differential operators arising in physical problems form an orthogonal basis — which is exactly the structure Fourier series exploits.

Working example: $L = d^2/dx^2$ with Dirichlet BCs. Take $L = d^2/dx^2$ acting on functions that vanish at the boundaries: $u(0) = u(1) = 0$. The eigenvalue problem (23) is

$$u''(x) + \lambda u(x) = 0, \qquad u(0) = u(1) = 0$$

For $\lambda > 0$, the general solution is

$$u(x) = c_1 \sin(\sqrt{\lambda}\,x) + c_2 \cos(\sqrt{\lambda}\,x)$$

The boundary condition $u(0) = 0$ forces $c_2 = 0$. The remaining condition $u(1) = 0$ gives $c_1 \sin(\sqrt{\lambda}) = 0$. We need $c_1 \neq 0$ to have a nontrivial eigenfunction, so $\sin(\sqrt{\lambda}) = 0$, i.e., $\sqrt{\lambda} = n\pi$ for $n = 1, 2, 3, \ldots$. The eigenvalues and eigenfunctions are therefore

$$\lambda_n = (n\pi)^2, \qquad u_n(x) = \sin(n\pi x), \qquad n = 1, 2, 3, \ldots \tag{24}$$

[2] The conventional form for differential eigenvalue problems is $Lu + \lambda u = 0$, slightly different from the matrix form $A\mathbf{v} = \lambda\mathbf{v}$ — the minus sign on λ is built into the convention. Despite the sign difference, u is still "the function that L scales," and λ is still "the corresponding eigenvalue."

These are exactly the sine basis functions of Section 1, up to the $\sqrt{2}$ normalization. *The sines we used to build Fourier series in Section 1 are the eigenfunctions of the second derivative with homogeneous Dirichlet boundary conditions.*

The other cases give nothing. For $\lambda = 0$, $u'' = 0$ has solution $u = ax + b$, and the BCs force $a = b = 0$. For $\lambda < 0$, the general solution is built from real exponentials, and again only the trivial solution satisfies both BCs. So all eigenvalues are positive, and the list (24) is complete.

Why the eigenfunctions are orthogonal. The orthogonality of the sines is no accident. For any two eigenfunctions u_m and u_n of $L = d^2/dx^2$ with the Dirichlet boundary conditions, integration by parts twice gives

$$\begin{aligned}\langle u_m'', u_n\rangle &= \int_0^1 u_m''(x)\, u_n(x)\, \mathrm{d}x \\ &= \big[u_m'\, u_n - u_m\, u_n'\big]_0^1 + \int_0^1 u_m(x)\, u_n''(x)\, \mathrm{d}x\end{aligned}$$

The boundary term $\big[u_m'\, u_n - u_m\, u_n'\big]_0^1$ vanishes because both u_m and u_n vanish at $x = 0$ and $x = 1$, leaving

$$\langle u_m'', u_n\rangle = \langle u_m, u_n''\rangle \tag{25}$$

In words: $L = d^2/dx^2$ "moves across" the inner product without penalty — we get the same answer whether we hit it on the left or the right.

Now use the eigenvalue equation: $u_m'' = -\lambda_m u_m$ and $u_n'' = -\lambda_n u_n$. Substituting into (25),

$$-\lambda_m \langle u_m, u_n\rangle = -\lambda_n \langle u_m, u_n\rangle$$

which rearranges to

$$(\lambda_n - \lambda_m)\langle u_m, u_n\rangle = 0$$

For $m \neq n$, the eigenvalues are different ($\lambda_n = (n\pi)^2$ are distinct positive numbers), so we must have $\langle u_m, u_n\rangle = 0$. *Eigenfunctions corresponding to distinct eigenvalues are automatically orthogonal.*

This argument explains the orthogonality we computed by hand back in Example 1.1. We did not pick the sine basis arbitrarily — it is, structurally, the basis of eigenfunctions of the differential operator that governs heat conduction in a slab with both ends held at the boundary temperature.

We now apply the same idea to a different differential operator and discover a third orthogonal basis.

Example 3.3 (Fourier–Bessel basis on $(0, 1)$)**.** Take the cylindrical Laplacian operator on $(0, 1)$,

$$Lu = \frac{1}{x}\frac{d}{dx}\left(x\,\frac{du}{dx}\right)$$

requiring u bounded at $x = 0$ and $u(1) = 0$ (these are the boundary conditions for, e.g., diffusion in a unit-radius cylinder with a fixed wall concentration). The eigenvalue problem $Lu + \lambda u = 0$ is

$$u'' + \frac{1}{x}u' + \lambda u = 0 \qquad \text{or, equivalently,} \qquad x^2u'' + xu' + \lambda x^2 u = 0$$

The substitution $z = \sqrt{\lambda}\,x$ turns this into Bessel's equation of order zero, so the general solution is

$$u(x) = c_1\, J_0(\sqrt{\lambda}\,x) + c_2\, Y_0(\sqrt{\lambda}\,x)$$

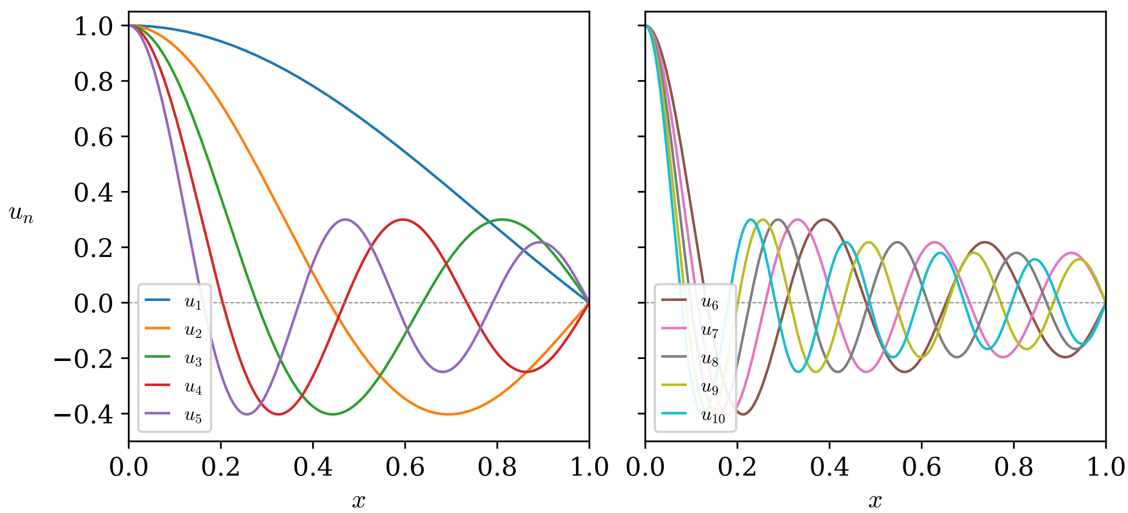

Figure 8: First ten Fourier–Bessel basis functions $u_n(x) = J_0\big(\sqrt{\lambda_n}\,x\big)$ on $[0, 1]$, where the λ_n are determined by $J_0(\sqrt{\lambda_n}) = 0$. Each u_n oscillates uniformly across the interval on its own length scale and vanishes at $x = 1$.

Boundedness at $x = 0$ forces $c_2 = 0$ since Y_0 blows up there. The remaining boundary condition $u(1) = 0$ then requires

$$J_0(\sqrt{\lambda_n}) = 0$$

which gives infinitely many eigenvalues $\lambda_1 < \lambda_2 < \cdots$. The first few have $\sqrt{\lambda_n} \approx 2.4048,\ 5.5201,\ 8.6537,\ \ldots$ (the positive zeros of J_0, see Table 1, top center panel). The eigenfunctions are

$$u_n(x) = J_0\Big(\sqrt{\lambda_n}\,x\Big), \qquad n = 1, 2, 3, \ldots \tag{26}$$

shown in Figure 8. Like the sines and Legendre polynomials, each successive u_n oscillates on a shorter length scale across the interval, and all of them vanish at $x = 1$.

These eigenfunctions form an orthogonal basis on $(0, 1)$ with respect to the *weighted* inner product

$$\langle u, v\rangle_x = \int_0^1 u(x)\,v(x)\,x\,\mathrm{d}x$$

The weight $w(x) = x$ comes from the $1/x$ prefactor in L, and $\langle u_m, u_n\rangle_x = 0$ for $m \neq n$ follows from the same integration-by-parts argument we used for the sines — with the weight x absorbing the $1/x$ when L moves across the inner product (see Exercise 4). The orthogonality relation and normalization (the latter requires a bit of Bessel-function identity work) are

$$\langle u_m, u_n\rangle_x = \int_0^1 J_0\Big(\sqrt{\lambda_m}\,x\Big)\,J_0\Big(\sqrt{\lambda_n}\,x\Big)\;x\;\mathrm{d}x = \tfrac{1}{2}\,J_1\Big(\sqrt{\lambda_n}\Big)^2\;\delta_{mn} \tag{27}$$

and the Fourier–Bessel series of a function f on $(0, 1)$ is

$$f(x) = \sum_{n=1}^{\infty} a_n\,u_n(x), \qquad a_n = \frac{\langle f, u_n\rangle_x}{\langle u_n, u_n\rangle_x} = \frac{2}{J_1\big(\sqrt{\lambda_n}\big)^2}\int_0^1 f(x)\,J_0\Big(\sqrt{\lambda_n}\,x\Big)\;x\;\mathrm{d}x \tag{28}$$

Two favorite functions in the Bessel basis. To check that this third basis works just like the others, we redo our two running examples on $(0, 1)$ in the Fourier–Bessel basis (28). Figure 9 shows the truncated Fourier–Bessel series for $f(x) = 1 - x$ and for $f(x) = \exp(-8x^2)$, with $N = 2, 5, 10$ terms. The Gaussian decays rapidly near $x = 1$ where it matches the basis (every u_n vanishes at $x = 1$) and converges quickly. For $f(x) = 1 - x$, with $f(1) = 0$ matching the basis but $f(0) = 1$ not constrained, convergence is reminiscent of the Section 1 sine series — somewhat slower but still effective with a modest number of terms.

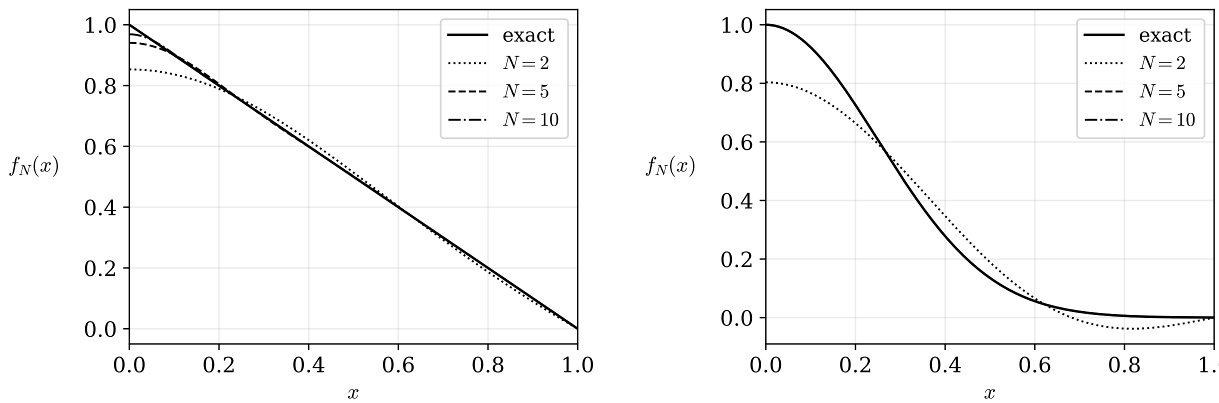

Figure 9: Fourier–Bessel series approximations on $(0, 1)$. Left: $f(x) = 1 - x$ with $N = 2, 5, 10$. Right: $f(x) = \exp(-8x^2)$ with the same truncations. Both use the basis $\{u_n(x)\}$ from (26).

The code below computes and plots this series for $f(x) = 1 - x$ and produces a result close to Figure 9 (left panel) in about twenty lines of either Python or MATLAB.

Python (NumPy / SciPy)

```
import numpy as np
import matplotlib.pyplot as plt
from scipy.special import j0, j1, jn_zeros
from scipy.integrate import quad

f = lambda x: 1.0 - x           # try also np.exp(-8*x**2)
N = 10
zeros = jn_zeros(0, N)          # sqrt(lambda_n), n = 1..N

a = np.zeros(N)                 # Fourier-Bessel coefficients
for n, sqrt_ln in enumerate(zeros):
    integrand = lambda x: f(x) * j0(sqrt_ln*x) * x
    a[n], _ = quad(integrand, 0.0, 1.0)
    a[n] *= 2.0 / j1(sqrt_ln)**2

x = np.linspace(0, 1, 400)
plt.plot(x, f(x), 'k-', label='exact')
for Nt in [2, 5, 10]:
    fN = sum(a[n]*j0(zeros[n]*x) for n in range(Nt))
    plt.plot(x, fN, label=f'N={Nt}')
plt.xlabel('x'); plt.legend(); plt.show()
```

MATLAB/Octave

```
N = 10;
sqrt_l = zeros(1, N);            % sqrt(lambda_n), n = 1..N
for n = 1:N
    sqrt_l(n) = fzero(@(x) besselj(0,x), (n-0.25)*pi);
end

f = @(x) 1 - x;                  % try also @(x) exp(-8*x.^2)

a = zeros(1, N);                 % Fourier-Bessel coefficients
for n = 1:N
    sn = sqrt_l(n);
    a(n) = 2/besselj(1,sn)^2 * ...
           integral(@(x) f(x).*besselj(0,sn*x).*x, 0, 1);
end

x = linspace(0, 1, 400);
plot(x, f(x), 'k-', 'DisplayName', 'exact'); hold on
for Nt = [2 5 10]
    fN = zeros(size(x));
    for n = 1:Nt
        fN = fN + a(n) * besselj(0, sqrt_l(n)*x);
    end
    plot(x, fN, 'DisplayName', sprintf('N=%d', Nt));
end
xlabel('x'); legend show; hold off
```

The key ingredients are the same in either language: a routine that returns the zeros of J_0 (`jn_zeros` in SciPy; `fzero` applied to `besselj(0, x)` in MATLAB) to get the $\sqrt{\lambda_n}$, a numerical quadrature routine (`quad` or `integral`) for the inner-product integrals, and built-in `j0`/`j1` (or `besselj`) calls to evaluate the basis. Switching to $f(x) = \exp(-8x^2)$ (the right panel of Figure 9) requires only changing the line that defines `f`.

A small aside on tooling: MATLAB does not (as of R2025) ship a built-in routine for the Bessel zeros, so the listing above resorts to `fzero`. Users on Octave (free, syntax-compatible with MATLAB) can call `gsl_sf_bessel_zero_J0` directly from the GSL package, since Octave inherits the well-tested zero-finding routines of the GNU Scientific Library.

A zoo of orthogonal bases. The eigenfunction idea is more general than the three bases we built and used here. Many classical orthogonal bases arise as eigenfunctions of an eigenvalue of the following form, known as the Sturm-Liouville equation,

$$\frac{d}{dx}\big[p(x)\,u'\big] + r(x)\,u + \lambda\,w(x)\,u = 0 \tag{29}$$

on a chosen domain, with homogeneous or boundedness boundary conditions. Different choices of the coefficients $p(x), r(x)$, the weight $w(x)$, and the domain produce different orthogonal bases of eigenfunctions, with the inner product weighted by w

$$\langle u, v\rangle_w = \int u(x)\,v(x)\,w(x)\;\mathrm{d}x$$

Note the Sturm-Liouville problem subsumes all three orthogonal bases illustrated in this handout: Fourier sine, Legendre polynomials, and Bessel functions J_ν. Table 3 lists these three and three more famous bases.

Basis	Domain	$p(x)$	$r(x)$	$w(x)$	Eigenfunctions
Fourier sine	$[0, 1]$	1	0	1	$\sin(n\pi x)$
Legendre polynomials	$[-1, 1]$	$1 - x^2$	0	1	$P_n(x)$
Bessel functions (order ν)	$(0, 1)$	x	$-\nu^2/x$	x	$J_\nu\left(\sqrt{\lambda_n}\, x\right)$
Chebyshev polynomials	$[-1, 1]$	$\sqrt{1 - x^2}$	0	$1/\sqrt{1 - x^2}$	$T_n(x)$
Hermite polynomials	$(-\infty, \infty)$	e^{-x^2}	0	e^{-x^2}	$H_n(x)$
Laguerre polynomials	$[0, \infty)$	$x\, e^{-x}$	0	e^{-x}	$L_n(x)$

Table 3: Six classical orthogonal bases. Each row gives the parameters p, r, w of the eigenvalue ODE (29) and the domain on which it lives. The first three rows are the bases used in this handout; the others are their famous cousins. The standard intervals $[0, 1]$ and $(0, 1)$ for the sine and Bessel rows are used for cleanliness; the rescaling trick from §3.1 adapts them to any other bounded domain.

Each problem "picks its own basis": the geometry, the differential equation, and the boundary conditions together determine the operator, and the operator hands you its orthogonal eigenfunctions. Heat conduction in a slab returns sines; in a cylinder, Bessel functions; in a sphere, Legendre polynomials and their two-variable generalization the spherical harmonics. In quantum mechanics, the harmonic oscillator gives Hermite polynomials and the hydrogen atom gives Laguerre polynomials. Chebyshev polynomials show up in numerical methods because their nonuniform weight $1/\sqrt{1 - x^2}$ produces approximations with very small worst-case error.

The lesson is that the "Fourier series" idea — representing a function as a sum of orthogonal basis functions weighted by inner-product projections — is genuinely universal. What changes from one application to the next is not the framework but the basis, and the basis is dictated by the differential equation we are solving. The unifying framework that makes all of this work is called Sturm–Liouville Theory; (Graham and Rawlings, 2022, Chap. 2) provides a more advanced treatment.

Exercises

Exercise 1 (Fourier sine series of a triangle wave).

Consider the triangle wave on $0 \le x \le 1$

$$f(x) = \begin{cases} x & \text{if } x < 1/2 \\ 1 - x & \text{if } x \ge 1/2 \end{cases}$$

Find the Fourier coefficients α_n for this function using the sine basis $\sin(n\pi x)$. Show that they decay as $1/n^2$ as $n \to \infty$. Plot $f(x)$ together with the truncated series

$$f_N(x) = \sum_{n=1}^{N} \alpha_n \sin(n\pi x)$$

for $N = 1, 3, 5, 10$ and comment on the convergence.

Exercise 2 (Fourier cosine series of a square wave).

The square wave on $0 \le x \le 1$,

$$g(x) = \begin{cases} +1 & 0 < x < 1/2 \\ -1 & 1/2 < x < 1 \end{cases}$$

is the derivative of the triangle wave f from Exercise 1. Differentiate f's sine series term by term, notice that the result is a cosine series for g,

$$g(x) = \sum_{n=1}^{\infty} b_n \cos(n\pi x)$$

write out the b_n explicitly, show that they decay as $1/n$, and plot $g_N(x)$ for $N = 2, 10, 50$.

Exercise 3 (Fourier series of a triangle wave).

Taken from (Graham and Rawlings, 2022, Exercise 2.10).

Consider the Fourier sine series approximation for the triangle wave depicted in Figure 10,

$$f_N(x) = \sum_{n=1}^{N} a_n \sin(n\pi x), \qquad x \in [0, 1]$$

(a) Find the coefficients a_n, $n = 1, 2, \ldots$. The integral formula

$$\int (mx + b) \sin(n\pi x) \, \mathrm{d}x = -\frac{mx + b}{n\pi} \cos(n\pi x) + \frac{m}{(n\pi)^2} \sin(n\pi x)$$

will save time on the integration by parts.

(b) Plot the function $f_N(x)$ for $N = 5, 10, 50$ to demonstrate convergence to $f(x)$. How many terms are required to obtain good accuracy?

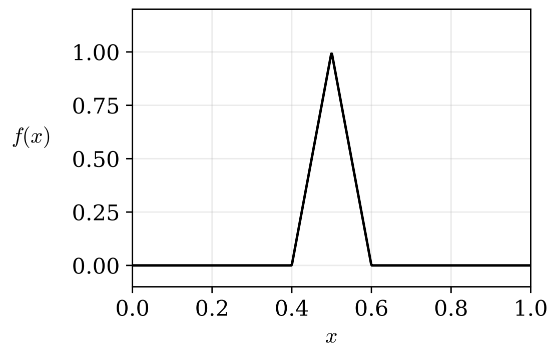

Figure 10: Narrow triangle wave on $[0, 1]$ with peak value 1 at $x = 1/2$ and support $[0.4, 0.6]$.

Exercise 4 (Orthogonality of the Fourier–Bessel basis).

The Fourier–Bessel eigenfunctions $u_n(x) = J_0(\sqrt{\lambda_n}\, x)$ on $(0, 1)$, with the $\sqrt{\lambda_n}$ the positive zeros of J_0, are eigenfunctions of the cylindrical Laplacian operator

$$Lu = \frac{1}{x}\frac{d}{dx}\left(x\,\frac{du}{dx}\right)$$

satisfying boundedness at $x = 0$ and $u(1) = 0$. In this exercise you show that they are orthogonal with respect to the weighted inner product $\langle u, v\rangle_x = \int_0^1 u(x)\, v(x)\, x \,\mathrm{d}x$, by following the same integration-by-parts strategy we used for the sine basis in Section 3.3.

(a) Show that for any two of the eigenfunctions u_m, u_n,

$$\langle Lu_m, u_n\rangle_x = \langle u_m, Lu_n\rangle_x$$

Hint: write out $\langle Lu_m, u_n\rangle_x$, cancel the $1/x$ factor in L against the x in the weight, then integrate by parts twice. The boundary conditions on u_m and u_n make all the boundary terms vanish.

(b) Use the result of part (a) and the eigenvalue equation $Lu_n = -\lambda_n u_n$ to conclude that

$$(\lambda_n - \lambda_m)\,\langle u_m, u_n\rangle_x = 0$$

and therefore $\langle u_m, u_n\rangle_x = 0$ whenever $m \neq n$.

Exercise 5 (Eigenfunctions of d^2/dx^2 under non-Dirichlet boundary conditions).

Section 3.3 of the handout works out the eigenpairs of $L = d^2/dx^2$ on $[0, 1]$ under homogeneous Dirichlet boundary conditions $u(0) = u(1) = 0$ and recovers the sine basis. In this exercise we change the boundary conditions and discover two more bases.

(a) **Neumann–Neumann.** Solve

$$u'' + \lambda u = 0, \qquad u'(0) = u'(1) = 0$$

Show that the eigenpairs are

$$\lambda_n = (n\pi)^2, \qquad u_n(x) = \cos(n\pi x), \qquad n = 0, 1, 2, \ldots$$

Note that $n = 0$ now contributes a nontrivial eigenfunction (the constant), in contrast to the Dirichlet case.

(b) **Dirichlet–Neumann (mixed).** Solve

$$u'' + \lambda u = 0, \qquad u(0) = 0, \quad u'(1) = 0$$

Show that the eigenpairs are

$$\lambda_n = \big((n+\tfrac{1}{2})\pi\big)^2, \qquad u_n(x) = \sin\!\big((n+\tfrac{1}{2})\pi x\big), \qquad n = 0, 1, 2, \ldots$$

(c) Conclude that *the basis is not a property of the operator alone* but of the operator together with its boundary conditions. Each of the three problems — Dirichlet–Dirichlet (the sines of Section 3.3), Neumann–Neumann, and Dirichlet–Neumann — produces a different orthogonal basis of $L^2(0,1)$.

Exercise 6 (Steady heat conduction in an insulated slab).

Repeat Example 1.2 but with both ends *insulated* instead of held at fixed temperature. The steady-state energy balance is

$$T'' = -f(x), \qquad T'(0) = T'(1) = 0$$

where $f(x) = F(x)/k$ is the scaled internal heat source. This problem requires the cosine basis from Exercise 5, not the sines.

(a) Define the orthonormal cosine basis on $[0, 1]$

$$\varphi_0(x) = 1, \qquad \varphi_n(x) = \sqrt{2}\cos(n\pi x), \qquad n = 1, 2, \ldots$$

and verify $\langle \varphi_m, \varphi_n \rangle = \delta_{mn}$. Note that $\varphi_n'' = -\lambda_n \varphi_n$ with $\lambda_n = (n\pi)^2$ for $n \geq 1$, and $\varphi_0'' = 0$ ($\lambda_0 = 0$).

(b) Expand T and f in this basis,

$$T(x) = \sum_{n=0}^{\infty} a_n\, \varphi_n(x), \qquad f(x) = \sum_{n=0}^{\infty} b_n\, \varphi_n(x)$$

Substitute into the ODE and match coefficients to show

$$a_n = \frac{b_n}{(n\pi)^2}, \quad n \geq 1 \qquad \text{and} \qquad b_0 = 0$$

The constraint $b_0 = 0$ is a *solvability condition*: the steady problem has no solution unless $\langle f, 1 \rangle = \int_0^1 f \,\mathrm{d}x = 0$. Interpret this physically.

(c) The constant mode a_0 is undetermined — the ODE plus Neumann BCs leaves T ambiguous up to an additive constant. Why?

(d) Solve the problem with $f(x) = x - \frac{1}{2}$. Show that $b_0 = 0$ (so the problem is solvable), compute the remaining coefficients, and verify that the resulting series sums to the closed-form solution

$$T(x) = c + \frac{x^2}{4} - \frac{x^3}{6}$$

obtained by direct integration of the ODE (where c is an arbitrary constant).

Exercise 7 (Gravity-driven flow down an inclined plate).

A Newtonian fluid of density ρ and viscosity μ flows in a thin layer of thickness L down a plane inclined at angle β from horizontal under gravity g (Figure 11). As you will learn in your transport class on fluids next year, in fully-developed flow with the wall at $z = 0$ and the free surface at $z = L$, the streamwise momentum balance describing the fluid velocity $u(z)$ is

$$\mu\, u''(z) = -\rho g \sin\beta, \qquad u(0) = 0, \quad u'(L) = 0$$

The first boundary condition is no-slip at the wall. The second is the absence of viscous shear at a gas-liquid free surface ($\tau_{xz} = \mu\, u'(L) = 0$, since the gas above exerts negligible shear stress).

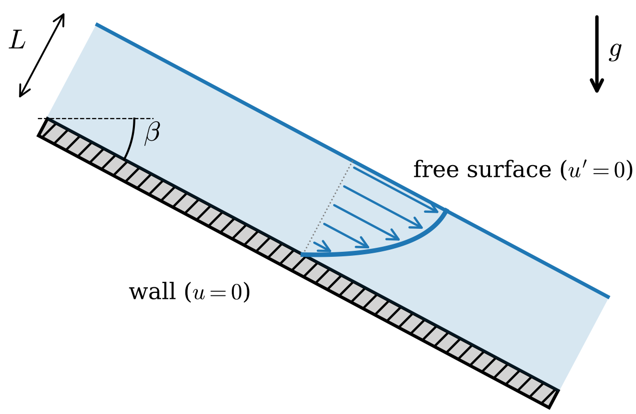

Figure 11: Gravity-driven flow of a Newtonian fluid down an inclined plate at angle β. The fluid layer has thickness L in the plate-normal direction. The boundary conditions are no-slip at the wall ($u = 0$ at $z = 0$) and no shear at the free surface ($u'(L) = 0$). The resulting velocity profile $u(z)$ is parabolic with its maximum at the free surface.

(a) Identify the boundary-condition pair as the Dirichlet–Neumann combination from Exercise 5(b), so that after rescaling $z' = z/L$ the relevant orthonormal basis on $[0, 1]$ is the half-integer sine family

$$\varphi_n(z') = \sqrt{2}\, \sin\!\big((n + \tfrac{1}{2})\pi z'\big), \qquad n = 0, 1, 2, \ldots$$

with eigenvalues $\lambda_n = ((n + \frac{1}{2})\pi)^2$. Verify $\langle \varphi_m, \varphi_n \rangle = \delta_{mn}$ and that $\varphi_n'' = -\lambda_n\, \varphi_n$.

(b) Solve the ODE directly by integration to obtain the parabolic profile

$$u(z) = \frac{\rho g \sin\beta}{2\mu}\left(2zL - z^2\right)$$

with maximum velocity $u_{\max} = u(L) = \rho g L^2 \sin\beta/(2\mu)$ at the free surface.

(c) Now solve the same problem by basis expansion in $\{\varphi_n\}$. Nondimensionalize with $z' = z/L$ and $\hat{u} = u\,\mu/(\rho g L^2 \sin\beta)$ to obtain

$$\hat{u}_{z'z'} = -1, \qquad \hat{u}(0) = 0, \quad \hat{u}'(1) = 0$$

Write $\hat{u}(z') = \sum_{n=0}^{\infty} a_n \varphi_n(z')$ and $-1 = \sum_{n=0}^{\infty} b_n \varphi_n(z')$, project to find the b_n, and use the recipe $a_n = b_n/\lambda_n$ from Example 1.2 to conclude

$$\hat{u}(z') = \frac{2}{\pi^3} \sum_{n=0}^{\infty} \frac{\sin\left((n+\frac{1}{2})\pi z'\right)}{(n+\frac{1}{2})^3}$$

Evaluate the truncated series with $N = 0$ (one term) at $z' = 1/2$ and check it against the closed form from part (b).

Exercise 8 (Effectiveness factor of a cylindrical catalyst pellet).

A long cylindrical catalyst pellet of radius R supports a first-order isothermal reaction with rate constant k (s^{-1}). The reactant species A has bulk concentration c_s at the pellet surface and diffuses inward with diffusivity D (Figure 12). At steady state the species balance in cylindrical coordinates is

$$D\,\frac{1}{r}\frac{d}{dr}\left(r\,\frac{dc}{dr}\right) = k\,c, \qquad c(R) = c_s, \qquad c \text{ bounded at } r = 0$$

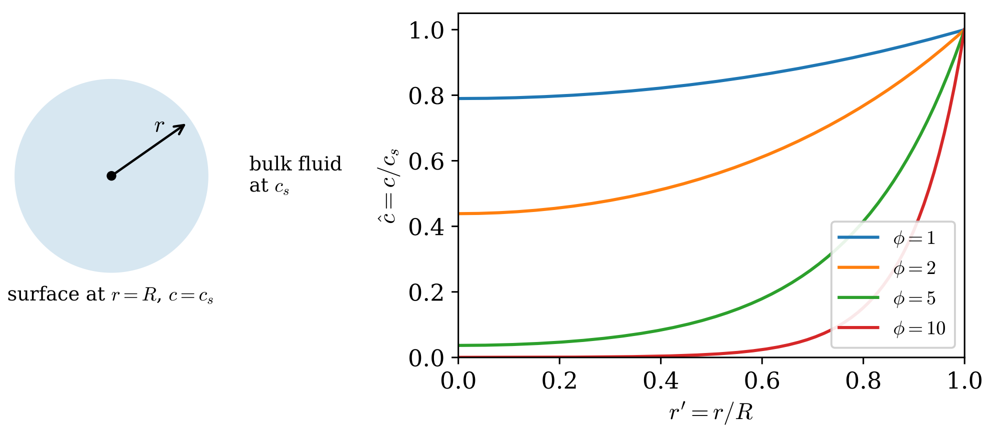

Figure 12: *Left:* cross-section of a long cylindrical catalyst pellet of radius R, immersed in a bulk fluid that holds the surface concentration at c_s. The reactant diffuses radially inward and is consumed by reaction throughout the pellet volume. *Right:* the dimensionless concentration profile $\hat{c}(r') = c(r)/c_s$ for several values of the Thiele modulus $\phi = R\sqrt{k/D}$. Small ϕ gives nearly uniform concentration (reaction-limited); large ϕ confines reactant to a thin shell near the surface (diffusion-limited).

(a) Nondimensionalize with $r' = r/R$ and $\hat{c} = c/c_s$ to obtain

$$\frac{1}{r'}\frac{d}{dr'}\left(r'\,\frac{d\hat{c}}{dr'}\right) = \phi^2\,\hat{c}, \qquad \hat{c}(1) = 1, \qquad \hat{c} \text{ bounded at } r' = 0$$

where $\phi = R\sqrt{k/D}$ is the *Thiele modulus*.

(b) This is the cylindrical $\nabla^2 y - y = 0$ (the minus-sign case in Table 1, middle column, bottom). Use the substitution $z = \phi r'$ to convert to the modified Bessel equation of order zero, conclude that the general solution is

$$\hat{c}(r') = A\,I_0(\phi r') + B\,K_0(\phi r')$$

and apply the two boundary conditions to obtain

$$\hat{c}(r') = \frac{I_0(\phi r')}{I_0(\phi)}$$

Plot $\hat{c}(r')$ for $\phi = 1, 2, 5, 10$ and compare to the right panel of Figure 12.

(c) The *effectiveness factor* η is the ratio of the actual reaction rate over the pellet to the rate that *would* obtain if the entire pellet sat at the surface concentration c_s,

$$\eta = \frac{\int_0^R k\, c(r)\, 2\pi r \; \mathrm{d}r}{k\, c_s\, \pi R^2} = 2 \int_0^1 \hat{c}(r')\, r' \; \mathrm{d}r'$$

Use the integral identity

$$\int_0^x z\, I_0(z) \; \mathrm{d}z = x\, I_1(x)$$

(which follows from $(z\, I_1(z))' = z\, I_0(z)$) to evaluate the integral and show that

$$\eta(\phi) = \frac{2\, I_1(\phi)}{\phi\, I_0(\phi)}$$

(d) Compute the limits $\phi \to 0$ and $\phi \to \infty$ using the small-argument expansions $I_0(\phi) \approx 1 + \phi^2/4$, $I_1(\phi) \approx \phi/2$ and the large-argument asymptotic $I_\nu(\phi) \sim e^\phi/\sqrt{2\pi\phi}$. Interpret each limit physically.

Exercise 9 (Orthogonality of Legendre polynomials from Sturm–Liouville).

The Legendre polynomials $P_n(x)$ on $[-1, 1]$ are eigenfunctions of the operator

$$Lu = \frac{d}{dx}\big[(1 - x^2)\, u'\big]$$

with eigenvalues $\lambda_n = n(n+1)$, in the sense that $LP_n + n(n+1)P_n = 0$. Following the same integration-by-parts strategy of Exercise 4, show that the P_n are mutually orthogonal with respect to the unweighted inner product $\langle u, v\rangle = \int_{-1}^1 u(x)\, v(x) \; \mathrm{d}x$.

(a) Show that for any two eigenfunctions u_m, u_n,

$$\langle Lu_m, u_n\rangle = \langle u_m, Lu_n\rangle$$

Hint: integrate by parts twice. Note that, unlike the Bessel and sine cases, no boundary condition on u_m or u_n is needed at $x = \pm 1$ — the factor $1 - x^2$ vanishes there and kills the boundary terms automatically.

(b) Use the result of part (a) and the eigenvalue equation $Lu_n = -n(n+1)u_n$ to conclude that

$$\big(n(n+1) - m(m+1)\big)\langle u_m, u_n\rangle = 0$$

and therefore $\langle u_m, u_n\rangle = 0$ whenever $m \neq n$.

Exercise 10 (Legendre Polynomials—The orthonormal viewpoint).

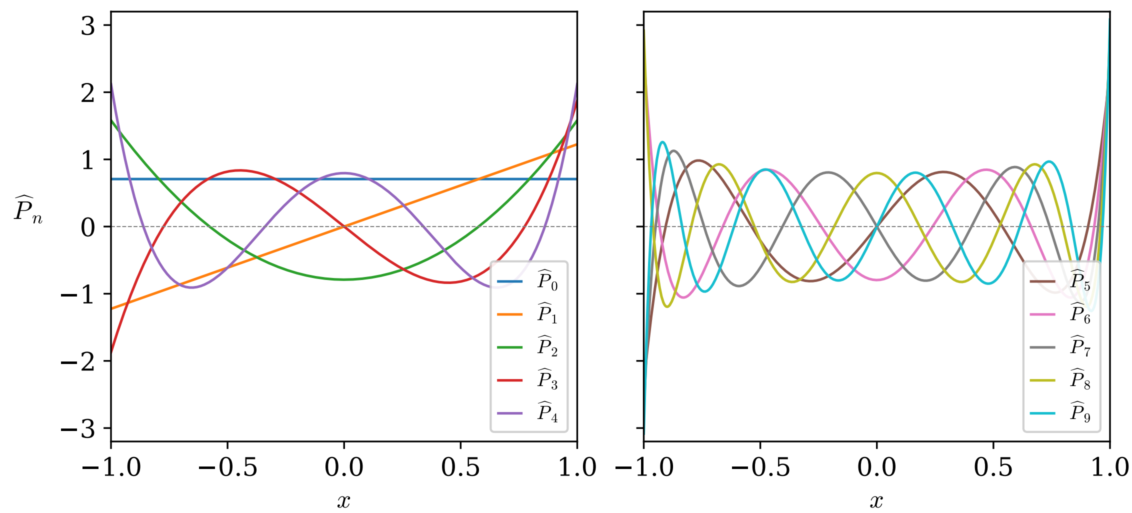

Figure 13: First ten orthonormal Legendre polynomials $\widehat{P}_0, \widehat{P}_1, \ldots, \widehat{P}_9$ on $[-1, 1]$, plotted with a common y-axis on both panels. Compare with Figure 6, which shows the same ten polynomials in the physicist's normalization $P_n(1) = 1$. The orthonormal scaling stretches the high-n polynomials by a factor of $\sqrt{(2n+1)/2}$, so the y-axis must now run from about -3.2 to $+3.2$ to fit $\widehat{P}_9$, and the lower-order curves look small by comparison.

The standard Legendre polynomials in this handout follow the "physicist's normalization" $P_n(1) = 1$, which gives the norm $\|P_n\|^2 = \frac{2}{2n+1}$. This norm depends on n, so the $\{P_n\}$ are orthogonal but not orthonormal. Define instead a rescaled basis $\widehat{P}_n$ by

$$\langle \widehat{P}_n, \widehat{P}_m \rangle = \int_{-1}^{1} \widehat{P}_n(x)\, \widehat{P}_m(x)\; \mathrm{d}x = \delta_{nm}$$

i.e., orthonormal with respect to the unweighted inner product on $[-1, 1]$. Figure 13 is the orthonormal analog of Figure 6; you will reproduce it in part (b) below and use it to argue about visualization.

(a) Show that the rescaling

$$\widehat{P}_n(x) = \sqrt{\tfrac{2n+1}{2}}\; P_n(x)$$

produces the desired orthonormal basis. Write out $\widehat{P}_0$ through $\widehat{P}_4$ explicitly and tabulate the endpoint value $\widehat{P}_n(1) = \sqrt{(2n+1)/2}$ for $n = 0, 1, \ldots, 9$.

(b) Reproduce Figure 13 from scratch: generate $P_n(x)$ via the three-term recurrence (20), multiply each by $\sqrt{(2n+1)/2}$, and plot $\widehat{P}_0, \ldots, \widehat{P}_9$ on $[-1, 1]$ with the same two-panel layout (left: $n = 0, \ldots, 4$; right: $n = 5, \ldots, 9$) and a common y-axis on both panels. Your output should agree visually with the figure shown above — this is the diagnostic that tells you the recurrence and the rescaling are both coded correctly.

(c) Compare Figure 13 side by side with Figure 6. Do you find either one more visually informative than the other? Discuss what each scaling emphasizes and what each one obscures. There is no right answer here — opinions vary among experienced readers about which normalization is preferable.

Exercise 11 (Plane Poiseuille flow).

A Newtonian fluid of viscosity μ flows steadily between two parallel, stationary, no-slip walls separated by a distance h under a constant streamwise pressure gradient $G = -dP/dx$. This is the simplest viscous internal-flow problem and a useful warmup for the porous-medium variant in Exercise 12.

Again, as you'll learn in your transport class, in fully-developed flow the streamwise momentum balance describing the fluid velocity $u(y)$ is

$$\mu\, u''(y) = -G, \qquad u(0) = 0, \quad u(h) = 0$$

(a) Integrate the ODE twice and apply the boundary conditions to obtain the parabolic profile

$$u(y) = \frac{G}{2\mu}\, y(h-y)$$

Sketch the profile (Figure 14).

(b) Compute the maximum velocity $u_{\max}$ (at the centerline $y = h/2$), the mean velocity $\bar{u} = (1/h)\int_0^h u\, dy$, and the volumetric flowrate per unit width $Q' = \bar{u}\, h$. Verify that $\bar{u} = (2/3)\, u_{\max}$.

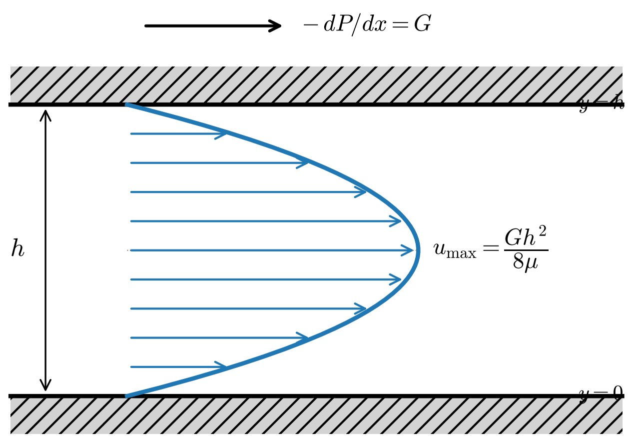

Figure 14: Plane Poiseuille flow: a Newtonian fluid driven by pressure gradient $-dP/dx$ between two stationary no-slip walls a distance h apart. The velocity profile is the parabola $u(y) = G\, y(h-y)/(2\mu)$ with maximum $u_{\max} = Gh^2/(8\mu)$ at the centerline.

Exercise 12 (Brinkman flow in a porous channel).

A Newtonian fluid of viscosity μ is forced through a slab of porous medium of thickness h and permeability k between two impermeable, no-slip walls by a constant streamwise pressure gradient $G = -dP/dx$. At a length scale where the porous structure can be treated as a continuum, the streamwise momentum balance is the *Brinkman equation*

$$\mu_e\, u''(y) - \frac{\mu}{k}\, u(y) = -G, \qquad u(0) = 0, \quad u(h) = 0$$

where μ_e is an effective viscosity that captures the macroscopic viscous diffusion of momentum across the porous medium. Brinkman flow interpolates between two familiar limits: ordinary Poiseuille flow when k is large (low Darcy resistance) and uniform Darcy plug flow when k is small (negligible viscous diffusion). Figure 15 plots the velocity profile across this transition.

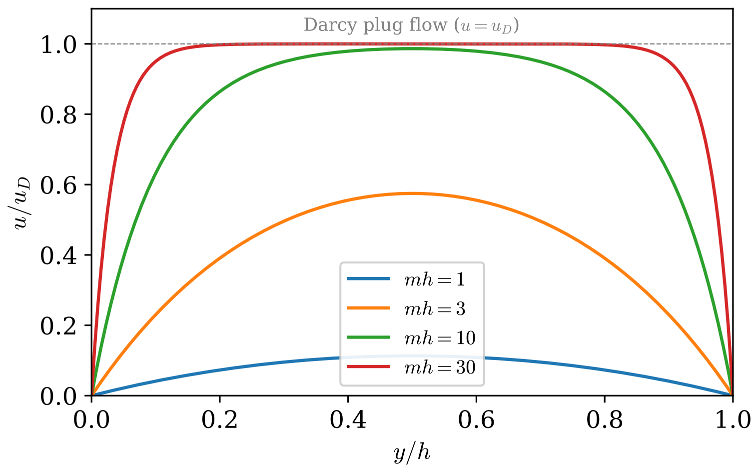

Figure 15: Brinkman velocity profile $u(y)/u_D$ as a function of y/h for several values of mh (the channel thickness measured in units of the Brinkman screening length $1/m$). Small mh recovers the plane-Poiseuille parabola (Exercise 11, scaled by $u_D = Gk/\mu$); large mh approaches uniform Darcy plug flow with thin Brinkman boundary layers near each wall.

(a) Define the inverse length $m = \sqrt{\mu/(k\mu_e)}$ (the reciprocal of the Brinkman screening length) and the Darcy velocity $u_D = Gk/\mu$. Show that the ODE rewrites as

$$u'' - m^2 u = -m^2 u_D$$

This is the rectangular $\nabla^2 y - y = 0$ form of Table 1 (left column, lower half) with a constant inhomogeneous term — so the homogeneous solutions are cosh, sinh and we add a particular solution that handles the source.

(b) Show that the constant $u_p = u_D$ is a particular solution. Combine it with the homogeneous part and apply the no-slip conditions to obtain the symmetric form

$$u(y) = u_D \left[1 - \frac{\cosh\big(m(y - h/2)\big)}{\cosh(mh/2)} \right]$$

Plot $u(y)/u_D$ versus y/h for $mh = 1, 3, 10, 30$ and compare to Figure 15. Hint: the problem is symmetric about $y = h/2$ (both BCs and the source are unchanged under $y \to h - y$), so the homogeneous correction must be even about the centerline; write it as $A\cosh(m(y - h/2))$ from the start.

Exercise 13 (Function expansion in the Fourier–Bessel and Legendre bases).

The handout demonstrates Fourier expansion mostly in the sine basis on $[0, 1]$. Here we practice the same projection-onto-orthogonal-basis procedure for the other two bases of Section 3.3.

(a) **Fourier–Bessel.** Compute the coefficients in the expansion of $f(r) = 1$ on $(0, 1)$ in the Fourier–Bessel basis $u_n(r) = J_0(\sqrt{\lambda_n}\, r)$, with $\sqrt{\lambda_n}$ the positive zeros of J_0. Use the integral identity

$$\int_0^1 r\, J_0(\sqrt{\lambda_n}\, r)\, \mathrm{d}r = \frac{J_1(\sqrt{\lambda_n})}{\sqrt{\lambda_n}}$$

(which follows from $(z\,J_1(z))' = z\,J_0(z)$) together with the orthogonality relation (27), and show that

$$a_n = \frac{2}{\sqrt{\lambda_n}\,J_1(\sqrt{\lambda_n})}$$

This is the Fourier–Bessel analog of the Fourier sine expansion of the constant function $f \equiv 1$, and the coefficient that appears in transient cylinder problems with uniform initial temperature.

(b) **Legendre.** Compute the coefficients in the expansion of $f(x) = |x|$ on $[-1, 1]$ in the Legendre basis $P_n(x)$. Use the orthogonality relation $\int_{-1}^{1} P_m P_n \,\mathrm{d}x = \frac{2}{2n+1}\,\delta_{mn}$, the symmetry of $|x|$ (only even n contribute), and the explicit formulas $P_0(x) = 1$, $P_2(x) = (3x^2 - 1)/2$, and $P_4(x) = (35x^4 - 30x^2 + 3)/8$ to obtain

$$a_0 = \tfrac{1}{2}, \qquad a_2 = \tfrac{5}{8}, \qquad a_4 = -\tfrac{3}{16}$$

Plot the truncated series $f_N(x) = \sum_{n=0}^{N} a_n P_n(x)$ for $N = 4$ and comment on the convergence.

Exercise 14 (Legendre polynomials by Gram–Schmidt).

The Legendre polynomials $\{P_n\}$ are the orthogonal basis on $[-1, 1]$ that arises from applying *Gram–Schmidt orthogonalization* to the monomials $\{1, x, x^2, x^3, \ldots\}$ with the unweighted inner product $\langle f, g\rangle = \int_{-1}^{1} f(x)\,g(x)\,\mathrm{d}x$ and choosing the standard normalization $P_n(1) = 1$. This exercise applies the Gram–Schmidt procedure — familiar from the orthogonalization of vectors in $\mathbb{R}^n$ — in the function-space setting.

(a) Apply Gram–Schmidt to $\{1, x, x^2, x^3\}$ (without normalization) to produce the four mutually orthogonal polynomials

$$q_0 = 1, \quad q_1 = x, \quad q_2 = x^2 - \tfrac{1}{3}, \quad q_3 = x^3 - \tfrac{3}{5}x$$

(b) Renormalize each q_n so that $q_n(1) = 1$ becomes $P_n(1) = 1$ and verify that the result reproduces the standard Legendre formulas

$$P_0(x) = 1, \quad P_1(x) = x, \quad P_2(x) = \tfrac{1}{2}(3x^2 - 1), \quad P_3(x) = \tfrac{1}{2}(5x^3 - 3x)$$

(c) Verify directly that $\int_{-1}^{1} P_2(x)P_3(x)\,\mathrm{d}x = 0$ (without using the general orthogonality theorem) as a sanity check on your construction.

(d) Check that the four polynomials P_0, P_1, P_2, P_3 produced above satisfy the three-term recurrence (20) $(n+1)P_{n+1} = (2n+1)\,x\,P_n - n\,P_{n-1}$ at $n = 1$ and $n = 2$ by direct substitution.

Exercise 15 (The Legendre recurrence reproduces the Gram–Schmidt sequence).

Exercise 14 verified the three-term recurrence (20)

$$(n+1)\,P_{n+1}(x) = (2n+1)\,x\,P_n(x) - n\,P_{n-1}(x)$$

on the first few Gram–Schmidt polynomials. Here you will show by induction that the recurrence reproduces the entire Gram–Schmidt sequence, not just the first few terms.

Suppose, for some $n \geq 1$, the polynomials $P_0, P_1, \ldots, P_n$ delivered by Gram–Schmidt satisfy

(i) $\langle P_j, P_k\rangle = 0$ for $0 \leq j < k \leq n$ (mutual orthogonality),

(ii) $P_k(1) = 1$ (the standard normalization),

(iii) $P_k(-x) = (-1)^k\, P_k(x)$ (parity matches the index),

(iv) $\|P_k\|^2 = \int_{-1}^{1} P_k^2\, \mathrm{d}x = 2/(2k+1)$ (the standard norm),

(v) the recurrence $(k+1)P_{k+1} = (2k+1)x\,P_k - k\,P_{k-1}$ holds for every $1 \le k \le n-1$ (vacuous when $n = 1$).

All five hold for $n = 3$ from Exercise 14 (parts (b)–(d) and direct computation of $\|P_k\|^2$). Define the next polynomial via the recurrence,

$$\widehat{P}_{n+1}(x) := \frac{(2n+1)\,x\,P_n(x) - n\,P_{n-1}(x)}{n+1}$$

The goal is to verify that $\widehat{P}_{n+1}$ has the same five properties at index $n+1$, so that the induction propagates and the recurrence holds for every $n \ge 1$. Verify in turn:

(a) $\widehat{P}_{n+1}$ has degree $n+1$ and parity $\widehat{P}_{n+1}(-x) = (-1)^{n+1}\,\widehat{P}_{n+1}(x)$.

(b) $\widehat{P}_{n+1}(1) = 1$.

(c) $\langle \widehat{P}_{n+1}, P_k\rangle = 0$ for $0 \le k \le n-2$. *Hint:* use the symmetry $\langle xP_n, P_k\rangle = \langle P_n, xP_k\rangle$ together with the inductive orthogonality of P_n.

(d) $\langle \widehat{P}_{n+1}, P_n\rangle = 0$. *Hint:* parity.

(e) $\langle \widehat{P}_{n+1}, P_{n-1}\rangle = 0$. *Hint:* use the symmetry, and apply the recurrence at index $k = n-1$ (hypothesis (v)) to expand $x\,P_{n-1}$. The result hinges on the norm formula (iv).

(f) Conclude that $\widehat{P}_{n+1}$ is the unique polynomial of degree $n+1$ that is orthogonal to $1, x, \ldots, x^n$ and takes the value 1 at $x = 1$ — i.e., it is exactly the next Gram–Schmidt polynomial P_{n+1}, so the recurrence holds at index n. By induction it holds for every $n \ge 1$.

Exercise 16 (Legendre's equation by induction on the recurrence).

The three-term recurrence (20)

$$(n+1)\,P_{n+1}(x) = (2n+1)\,x\,P_n(x) - n\,P_{n-1}(x)$$

together with the seeds $P_0(x) = 1$, $P_1(x) = x$ generates every Legendre polynomial. In this exercise you will show, by induction on n, that every P_n produced by this recurrence satisfies

$$LP_n + n(n+1)P_n = 0, \qquad Lu = \frac{d}{dx}\big[(1-x^2)\,u'\big]$$

i.e., that P_n is an eigenfunction of L with eigenvalue $\lambda_n = n(n+1)$. This is the fact taken as given in Exercise 9.

The induction needs a second identity to close, so we carry it along in tandem,

$$(1-x^2)\,P_n'(x) = n\big[P_{n-1}(x) - x\,P_n(x)\big] \qquad (\star) \tag{30}$$

(a) (Base cases.) Verify directly from $P_0 = 1$ and $P_1 = x$ that $LP_0 = 0$, $LP_1 + 2P_1 = 0$, and that $(\star)$ holds at $n = 1$.

(b) (Derivative recurrence.) Assume the inductive hypothesis: $LP_k + k(k+1)P_k = 0$ and ($\star$) at index k, for all $1 \le k \le n$. Solve ($\star$) at index n for P_{n-1}, differentiate, and use $LP_n = -n(n+1)P_n$ to conclude

$$P'_{n-1}(x) = x\,P'_n(x) - n\,P_n(x)$$

Substitute this into the differentiated recurrence to obtain

$$P'_{n+1}(x) = (n+1)\,P_n(x) + x\,P'_n(x)$$

(c) (Step ($\star$) forward.) Multiply the result of part (b) by $(1-x^2)$, apply ($\star$) at index n on the right-hand side, and use the recurrence (20) to eliminate the P_{n-1} term in favor of P_{n+1}. Conclude that ($\star$) holds at index $n+1$

$$(1-x^2)\,P'_{n+1}(x) = (n+1)\big[P_n(x) - x\,P_{n+1}(x)\big]$$

(d) (Step the eigenvalue equation forward.) Differentiate ($\star$) at index $n+1$ to compute LP_{n+1}. Eliminate xP'_{n+1} using part (b), eliminate $(1-x^2)P'_n$ using ($\star$) at index n, and eliminate $(2n+1)xP_n$ using the recurrence, to obtain

$$LP_{n+1} + (n+1)(n+2)\,P_{n+1} = 0$$

This closes the induction, and P_n is an eigenfunction of L with eigenvalue $n(n+1)$ for every $n \ge 0$.

References

M. Abramowitz and I. A. Stegun, editors. *Handbook of Mathematical Functions*. Dover, New York, 1964.

M. D. Graham and J. B. Rawlings. *Modeling and Analysis Principles for Chemical and Biological Engineers*. Nob Hill Publishing, Santa Barbara, CA, 2nd, paperback edition, 2022. 560 pages, ISBN 978-0-9759377-6-1.